To Günther

SINGULARITY-FREE METHODS FOR AIRCRAFT FLIGHT PATH OPTIMIZATION USING EULER ANGLES AND QUATERNIONS

BY

HANS-JOACHIM WUENSCHE

THESIS

Presented to the Faculty of the Graduate School of

The University of Texas at Austin

in Partial Fulfillment

of the Requirements

for the Degree of

MASTER OF SCIENCE IN ENGINEERING

THE UNIVERSITY OF TEXAS AT AUSTIN

May, 1982

ACKNOWLEDGEMENTS

I am most grateful for the positive help and encouragement that I have recieved during my studies at the University of Texas. In particular I wish to thank Dr. Hull for his careful guidance, ready advice and constructive criticism given in many hours of enjoyable and profitable discussions. Despite his busy schedule Dr. Speyer found time to give me important directions at critical points in my work. Also, I appreciate the generosity of the Fulbright Commission, which made possible the exciting experience of this stay in the United States.

January 11, 1982

TABLE OF CONTENTS

LIST OF SYMBOLS

Symbol	Definition
A	aerodynamic force
a	acceleration of aircraft with respect to earth
C_L	lift coefficient
D	drag
g	acceleration of gravity
h	altitude above msl
$\hat{i},\hat{j},\hat{k}$	coordinate system unit vectors
$\hat{I},\hat{J},\hat{K}$	unit vectors of an inertial reference system
L	lift
m	mass
p,q,r	angular velocity components
Q	sideforce
$\underline{Q}$	quaternion
T	thrust
t	time
V	velocity
W	weight
X,Y,Z	coordinates of aircraft c.g. in the fixed-earth frame

Symbol	Definition
α	aircraft angle of attack
β	mass flow rate of fuel
γ	velocity pitch angle; often also called flight path angle
ε	thrust angle of attack
ε_o	thrust angle of incidence
$\hat{\varepsilon}$	unit vector in rotation axis direction
θ	set 2 velocity pitch angle (Section III) rotation angle around the Euler axis (Section IV)
μ	velocity roll angle; also called bank angle
μ^*	dummy control
ν	thrust sideslip angle
π	engine power setting
σ	aircraft sideslip angle
τ	normalized time
ϕ	set 2 velocity roll angle
χ	velocity yaw angle; also called the heading angle
ψ	set 2 velocity yaw angle
Ω	angular velocity measured in the reference system
ω	angular velocity measured in the wind axes system

Symbol	Definition

Superscripts :

$\bar{q}$ - vector, having the elements q_1, q_2, q_3

$\dot{x}$ - derivative of x with respect to the time t

x' - derivative of x with respect to the normalized time τ

$\underline{Q}^*$ - quaternion conjugate

$\underline{Q}^{-1}$ - quaternion inverse

$[.,...,.]^T$ - vector

Subscripts :

$\underline{Q}$ - quaternion, having the elements q_o, q_1, q_2, q_3

w - wind axes system

h - local horizon system

v - vertical reference system

Miscellaneous:

$|\gamma|$ - absolute value of the scalar γ

$|\bar{\omega}|$ - length of the vector $\bar{\omega}$

$||\underline{Q}||$ - norm of the quaternion $\underline{Q}$

LIST OF FIGURES

LIST OF FIGURES, CONT'D

SECTION I

INTRODUCTION

The commonly-used general equations of motion for an aircraft in flight over a flat, nonrotating earth have a singularity for flight path angles of plus or minus 90 deg. This singularity leads to the fact that these equations of motion may only be integrated for flight path angles of up to +/- (90-ε) deg, where ε is dependent on the accuracy of the computations involved. These trajectories are referred to here as trajectories of the first class. Second-class trajectories, i.e. those where the flight path angle merely passes through +/- 90 deg, or third-class trajectories where the flight path angle may stay at +/- 90 deg for any finite amount of time are, therefore, not permissible with this set of equations of motion. There are many optimizaton problems, however, which have second- or third-class trajectories as their solution. The solution to the minimum-time-to-turn problem, for instance, is the so-called "Split-S" maneuver, provided the initial speed is below the corner speed [Well]. In the "Split-S" maneuver the aircraft starts out in straight and level flight, upside down. The pilot then pulls through until the aircraft achieves level flight again, where the airplane is now flying right side up in the opposite direction. This would be a trajectory of the second class. Other optimization problems, for instance the problem of restarting a jet engine in minimum time, may include vertical dives or vertical climbs, i.e. third-class trajectories.

The purpose of this work is to rewrite the equations of motion such that even third-class trajectories can be optimized with the current parameter optimization methods. At first the commonly used coordinate systems and Euler angles are presented in Section II. It will be realized that the definition of the Euler angles introduces additional singularities. A short derivation of the commonly-used equations of motion follows for comparison and better understanding of the later derived sets of equations of motion. Section II closes with a reduction of the optimal control problem to a parameter optimization problem. Some characteristic properties and assumptions of the parameter optimization problem are pointed out along with the necessary equations and conditions needed to solve it.

Section III introduces several methods that allow integration of second- and third-class trajectories as long as some restrictions are imposed on the allowable trajectories. The first method is the so-called inertial-acceleration method. It is based on the idea that the velocity yaw angle and the velocity pitch angle can be replaced by the velocity components as measured in an inertial reference frame. The so-called two-system method is derived next. It employes the idea of having two sets of equations of motion derived in different reference frames, and thus, having their singularities at different points. In detailed discussions the problems that appear with both methods are explained, and solutions are presented, the emphasis always being on the use of these equations with optimization methods. Section III also includes a method that allows integration of third -

class trajectories as long as they can be flown in the vertical plane. This method results directly from the commonly-used equations of motion after removing a restriction on the flight path angle. Because all methods of Section III have still the bank angle as the control, they are referred to here as Euler-angle methods.

Section IV presents the quaternion method. Although this method has been investigated first, it is presented last because it yields the best overall solution and because many details and improvements were not found until the other methods were analyzed. Understanding the Euler-angle methods will also help in understanding the properties of the quaternion method. Because the available literature on quaternions is either complex or erroneous, the quaternion is covered in much detail. The concept of the quaternion is explained, and the rules of quaternion algebra are stated in the first two sections. Next, some necessary relationships are developed. It will then be rather straightforward to derive the actual equations of motion. How to use the quaternion method for parameter optimization methods is emphasized in the following sections.

A short conclusion is drawn in Section V. Readers wishing some quick information about the results of this study should, however, first read the comparison section and the discussion section at the end of Sections III and IV, respectively, before reading the conclusion.

A second two-system method is presented in Appendix A because it seems promising but has not been tested numerically. Appendix B and Appendix C contain parts of derivations that have been ommitted from Section IV because they simply constitute elaborate algebraic manipulations.

SECTION II

FUNDAMENTALS

1. Coordinate Systems and Euler Angles

When analyzing flight performance of aircraft flying at small velocities with respect to the escape velocity over short ranges, the earth can be regarded as ideally flat and nonrotating. Under these assumptions four coordinate systems are usually defined: the ground axes system E X Y Z, the local horizon system O x_h y_h z_h, the wind axes system O x_w y_w z_w, and the body axes system O x_b y_b z_b [Miele]. How these coordinate systems are related to each other can be seen in Figures 1 through 3. The local horizon axes are always parallel to the ground axes, and the body axes are related to the wind axes through the angle of attack α and the sideslip angle σ .

The two coordinate systems of main interest are the local horizon system and the wind axes system. These two systems may be related to each other in several ways. Usually, three consecutive rotations are used to rotate the local horizon system into the wind axes system. These three rotations are carried out through three rotation angles, which are called the Euler angles. However, since the three rotation angles depend on the order in which the rotations are performed, one specific rotation sequence has to be defined. The commonly-used sequence in flight mechanics is given by the velocity-yaw-pitch-roll Euler angles, which are found by rotating the reference

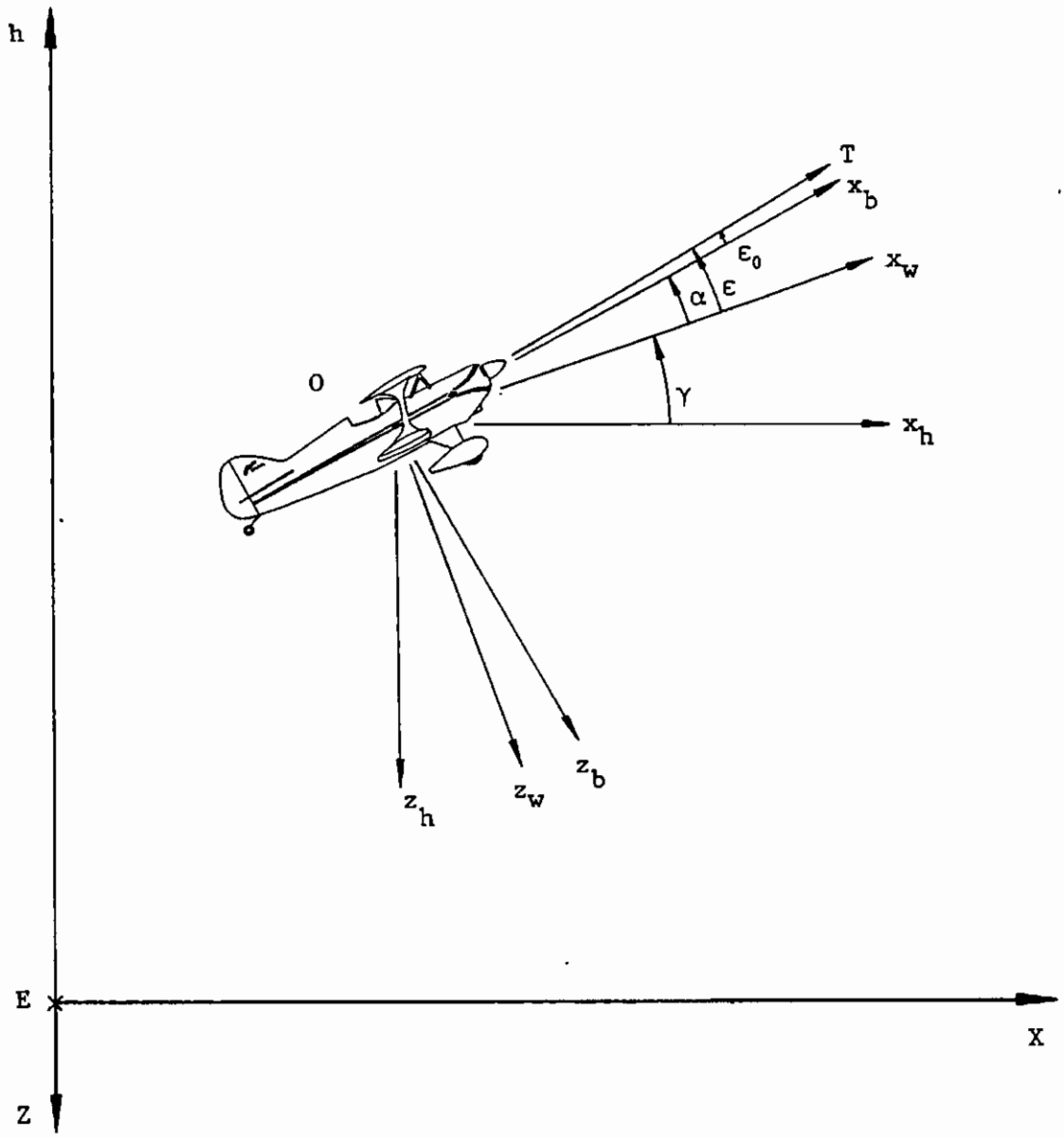

Figure 1 : Flight Path Angle γ, Aircraft Angle of Attack α, and Thrust Angle of Attack ε

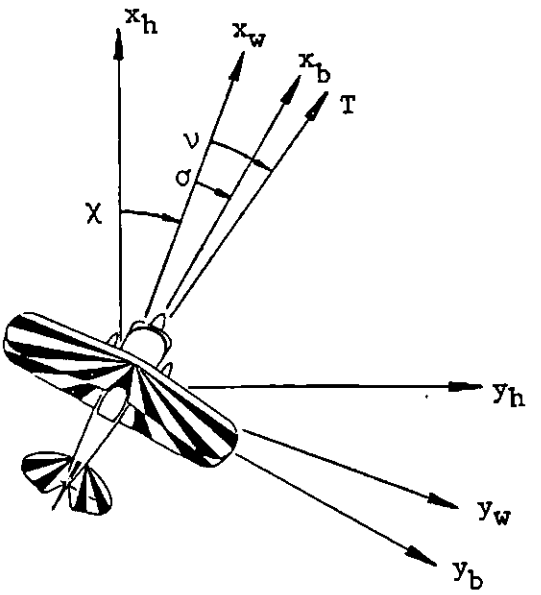

Figure 2 : Velocity Yaw Angle χ, Sideslip Angle σ, and Thrust Sideslip Angle ν

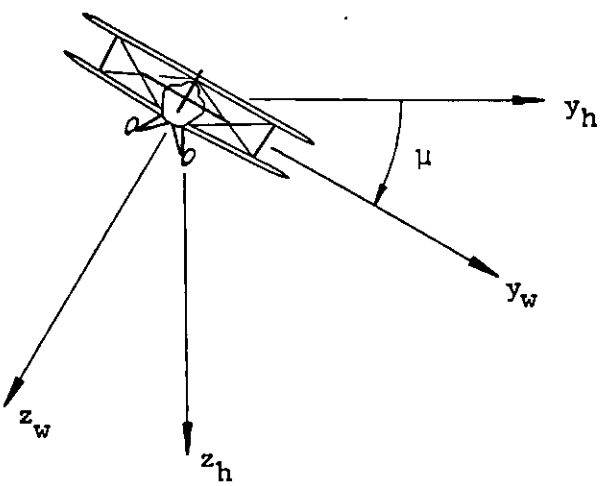

Figure 3 : Velocity Roll Angle μ

system first around its z-axis into system 1 (through the velocity yaw angle χ), then system 1 around its y_1-axis into system 2 (through the velocity pitch angle γ), and finally system 2 around its x-axis into the wind axes system (getting the velocity roll angle μ). Hence, the velocity yaw and velocity pitch angles define the orientation of the aircraft velocity vector with respect to the local horizon system, whereas the velocity roll angle μ describes the angular position of the aircraft around the velocity vector.

Although necessary, one particular rotation sequence is not sufficient for getting a one-to-one relationship between the set of possible rotation angles and the set of possible aircraft attitudes. For instance, an upside down attitude in level flight (χ = 0 deg, γ = 0 deg and μ = 180 deg) may also be achieved by yawing 180 deg and then pitching 180 deg, i.e. χ = 180 deg, γ = 180 deg and μ = 0 deg. To circumvent this ambiguity, the velocity pitch angle γ is restricted to +/- 90 deg, whereas χ and μ go from - 180 deg to + 180 deg. However, this restriction on γ leads to singularities in χ and μ whenever γ exceeds + 90 deg or - 90 deg during some second- or third-class trajectory. For the above mentioned "Split-S" maneuver, for instance, it is seen that χ = 0 deg and μ = 180 deg for the first part of the maneuver until the flight path angle hits - 90 deg. At that point χ jumps from 0 deg to 180 deg and μ jumps from 180 deg to 0 deg because the aircraft is flying right side up in the opposite direction for the second part of the maneuver (Figure 4).

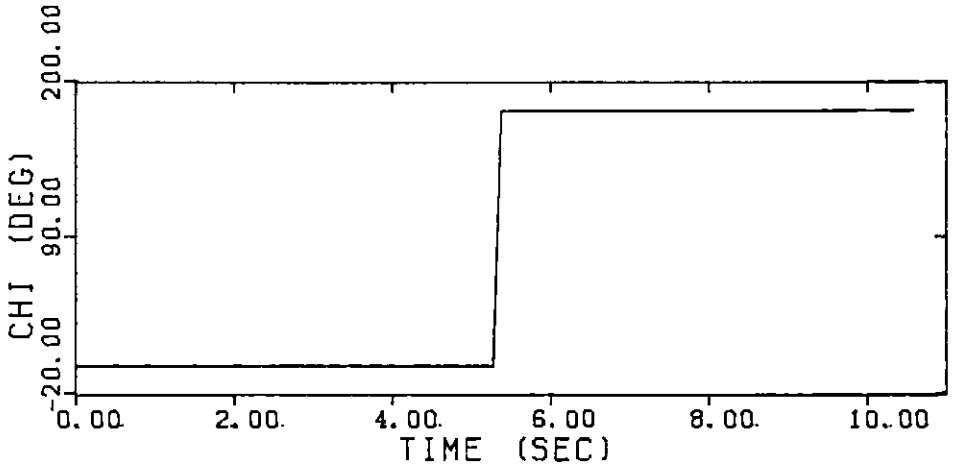

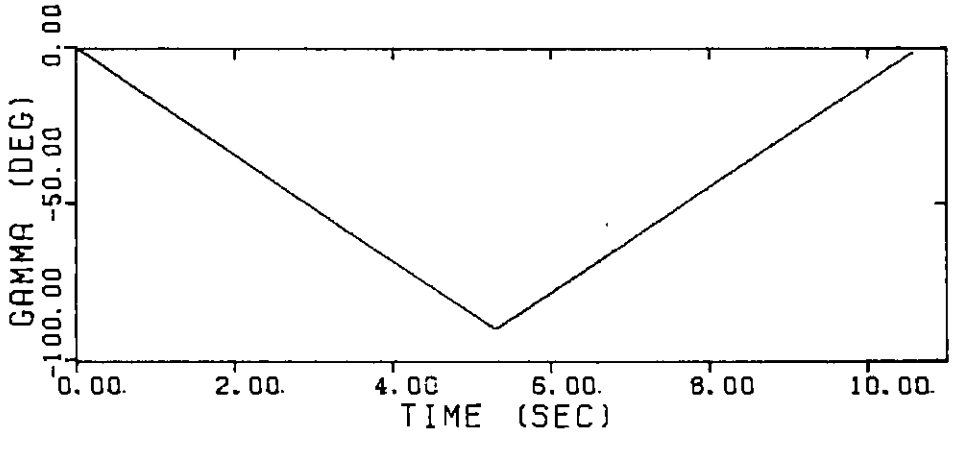

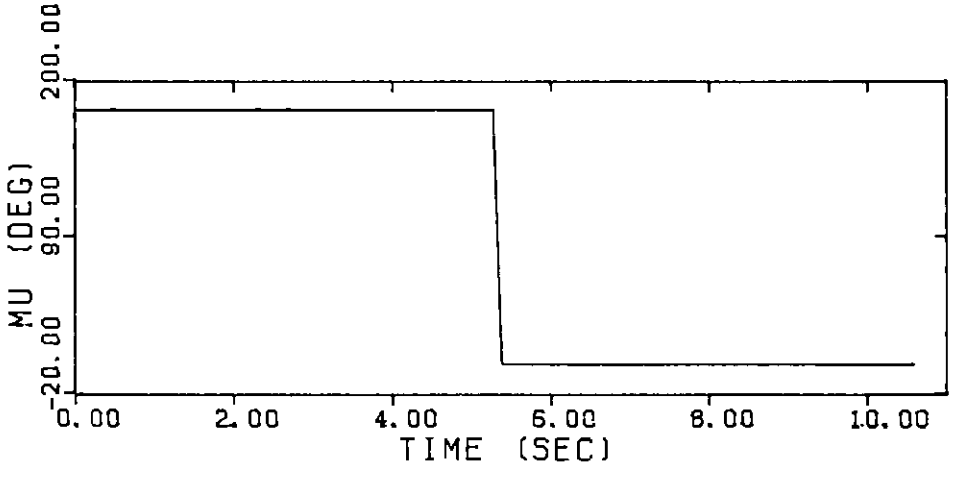

Figure 4 : Euler Angle Histories for the Split-S Maneuver

2. The Commonly-Used Equations of Motion

The dynamical equation for a vehicle in flight over a flat, nonrotating earth is given by

$$\bar{T} + \bar{A} + m\bar{g} = m\bar{a} = m\frac{d\bar{V}}{dt} \tag{2.1}$$

where

$\bar{T}$ - thrust

$\bar{A}$ - aerodynamic force

m - mass

$\bar{g}$ - acceleration of gravity

$\bar{a}$ - acceleration of aircraft with respect to earth

t - time

and where

$$\bar{V} = \frac{d}{dt}\overline{EO} \tag{2.2}$$

denotes the velocity of the aircraft with respect to the earth, E and O being the origin of the earth-based system and the local horizon system, respectively.

With $\bar{V} = V\hat{i}_w$ and $\overline{EO} = X\hat{i}_h + Y\hat{j}_h + Z\hat{k}_h$, it follows from Eq. (2.2) that

$$V\hat{i}_w = \dot{X}\hat{i}_h + \dot{Y}\hat{j}_h - \dot{h}\hat{k}_h \tag{2.3}$$

where $Z = -h + \text{const}$ has been used. Next, the relationship between the wind axes system and the local horizon system is given by the

direction cosine matrix

$$\begin{vmatrix} \hat{i}_w \\ \hat{j}_w \\ \hat{k}_w \end{vmatrix} = \begin{vmatrix} \cos\gamma\cos\chi & \cos\gamma\sin\chi & -\sin\gamma \\ \sin\mu\sin\gamma\cos\chi - \cos\mu\sin\chi & \sin\mu\sin\gamma\sin\chi + \cos\mu\cos\chi & \sin\mu\cos\gamma \\ \cos\mu\sin\gamma\cos\chi + \sin\mu\sin\chi & \cos\mu\sin\gamma\sin\chi - \sin\mu\cos\chi & \cos\mu\cos\gamma \end{vmatrix} \begin{vmatrix} \hat{i}_h \\ \hat{j}_h \\ \hat{k}_h \end{vmatrix} \tag{2.4}$$

Since the transformation matrix, or direction cosine matrix, is orthogonal, its inverse equals its transpose so that

$$\begin{vmatrix} \hat{i}_h \\ \hat{j}_h \\ \hat{k}_h \end{vmatrix} = \begin{vmatrix} \cos\gamma\cos\chi & \sin\mu\sin\gamma\cos\chi - \cos\mu\sin\chi & \cos\mu\sin\gamma\cos\chi + \sin\mu\sin\chi \\ \cos\gamma\sin\chi & \sin\mu\sin\gamma\sin\chi + \cos\mu\cos\chi & \cos\mu\sin\gamma\sin\chi - \sin\mu\cos\chi \\ -\sin\gamma & \sin\mu\cos\gamma & \cos\mu\cos\gamma \end{vmatrix} \begin{vmatrix} \hat{i}_w \\ \hat{j}_w \\ \hat{k}_w \end{vmatrix} \tag{2.5}$$

This reduces Eq. (2.3) to the kinematic relationships

$$\begin{aligned} \dot{X} &= V\cos\gamma\cos\chi \\ \dot{Y} &= V\cos\gamma\sin\chi \\ \dot{h} &= V\sin\gamma \end{aligned} \tag{2.6}$$

The dynamical relationship (2.1) is broken down into scalar equations by expressing all terms in the wind axes system. If ν denotes the thrust sideslip angle and ε the thrust angle of attack analogous to σ and α, the thrust is given by

$$\overline{T} = T\,(\cos\varepsilon\cos\nu\,\hat{i}_w + \cos\varepsilon\sin\nu\,\hat{j}_w - \sin\varepsilon\,\hat{k}_w) \tag{2.7}$$

The aerodynamic force A is written as

$$\bar{A} = - D\hat{i}_w - Q\hat{j}_w - L\hat{k}_w \tag{2.8}$$

where D is the drag, Q the side force and L the lift. From $\bar{g} = g\hat{k}_h$ and Eqs. (2.5), it follows that

$$\bar{g} = g\,(-\sin\gamma\,\hat{i}_w + \sin\mu\cos\gamma\,\hat{j}_w + \cos\mu\cos\gamma\,\hat{k}_w) \tag{2.9}$$

Next, the acceleration can be written as

$$\frac{d}{dt}(V\hat{i}_w) = \dot{V}\hat{i}_w + V\frac{d\hat{i}_w}{dt} \tag{2.10}$$

With Poisson's formula

$$\frac{d}{dt}\hat{i}_w = \bar{\omega} \times \hat{i}_w\ , \tag{2.11}$$

where the angular velocity $\bar{\omega}$ of the aircraft with respect to the local horizon system is given by

$$\bar{\omega} = p_w\hat{i}_w + q_w\hat{j}_w + r_w\hat{k}_w\ , \tag{2.12}$$

Eq. (2.10) results in

$$\frac{d\bar{V}}{dt} = \dot{V}\,\hat{i}_w + V\,r_w\hat{j}_w - V\,q_w\hat{k}_w \tag{2.13}$$

Consequently, Eq. (2.1) combined with Eqs. (2.7), (2.8), (2.9) and (2.13) leads to the scalar dynamic relationships

$$\begin{aligned} m\dot{V} &= T\cos\varepsilon\cos\nu - D - mg\sin\gamma \\ mVr_w &= T\cos\varepsilon\sin\nu - Q + mg\sin\mu\cos\gamma \\ mVq_w &= T\sin\varepsilon + L - mg\cos\mu\cos\gamma \end{aligned} \tag{2.14}$$

The velocity roll rate p_w, pitch rate q_w and yaw rate r_w are related to the Euler angle rates $\dot{\mu}$, $\dot{\gamma}$ and $\dot{\chi}$ through the equations

$$\begin{aligned} p_w &= \dot{\mu} - \dot{\chi} \sin\gamma \\ q_w &= \dot{\gamma} \cos\mu + \dot{\chi} \sin\mu \cos\gamma \\ r_w &= -\dot{\gamma} \sin\mu + \dot{\chi} \cos\mu \cos\gamma \end{aligned} \tag{2.15}$$

which are found by knowing that χ occurs about the $\hat{k}$ - axis, γ occurs about the $\hat{j}_1$ - axis and μ about the $\hat{i}_2$ - axis. Combining Eqs. (2.14) with (2.15), solving for $\dot{\chi}$ and $\dot{\gamma}$, and repeating the kinematic equations (2.6) yields the equations of motion

$$\begin{aligned} \dot{X} &= V \cos\gamma \cos\chi \\ \dot{Y} &= V \cos\gamma \sin\chi \\ \dot{h} &= V \sin\gamma \\ m\dot{V} &= T \cos\varepsilon \cos\nu - D - mg \sin\gamma \\ mV\dot{\chi} &= \frac{1}{\cos\gamma} \{T (\cos\varepsilon \sin\nu \cos\mu + \sin\varepsilon \sin\mu) + L \sin\mu - Q \cos\mu\} \\ mV\dot{\gamma} &= T (\sin\varepsilon \cos\mu - \cos\varepsilon \sin\nu \sin\mu) + L \cos\mu + Q \sin\mu - mg \cos\gamma \\ \dot{m} &= -\beta \end{aligned} \tag{2.16}$$

where β is the mass flow rate of fuel.

This set of equations has far more variables than equations. However, since L, D, Q, T and β are functions of h, V, α, ε, σ, ν and π, where π is the engine power setting, the independent variables narrow down to μ, α, ε, σ, and π. Hence, this system of equations has six degrees of freedom. For most cases it is feasible to set the sideslip angle σ and the thrust sideslip angle ν to zero. If the

engine is now assumed to be fixed with respect to the aircraft, then $\varepsilon_o = \varepsilon - \alpha = \text{const}$, and ε becomes a function of α and is thus eliminated as the control. This leaves the bank angle μ , the angle of attack α , and the power setting π as controls. Often the lift-coefficient C_L is used as control instead of α .

Eqs. (2.16) show why this set of equations of motion is not suitable for second-class trajectories. As γ approaches +/- 90 deg, the differential equation for χ starts "blowing up" or, if $\dot{\chi}$ is zero as in a Split-S maneuver or in a loop, the differential equation for χ becomes undetermined. Because of the singularities in χ and μ at $\gamma = +/- 90$ deg, as discussed in the previous section, this problem cannot be cured by choosing the integration steps such that $\cos\gamma$ does not get small enough to impose problems on $\dot{\chi}$ or by extrapolating $\dot{\chi}$ over the period it would be undefined.

It is possible, however, to integrate reasonably close to the vertical attitude after using regularization. This is done by multiplying both sides of Equations (2.16) by $\cos\gamma$, which removes the $\cos\gamma$ from the denominator of the $\dot{\chi}$ equation. The mass equation, for instance, would change to

$$\frac{dm}{dt}\cos\gamma = -\beta\cos\gamma \qquad (2.17)$$

or, with $d\tau = dt/\cos\gamma$, to

$$\frac{dm}{d\tau} = -\beta\cos\gamma \qquad (2.18)$$

Thus, all equations are now differentiated with respect to the new variable τ instead of the time t. This allows a constant integration stepsize $d\tau$ all the way to $\gamma = +/- 90$ deg, which, however, is never reached because dt is constantly decreased according to the equation $dt = d\tau \cos\gamma$. To keep track of the time t , the differential equation

$$\frac{dt}{d\tau} = \cos\gamma \tag{2.19}$$

is integrated along with the rest of the equations of motion.

3. Reduction of the Optimal Control Problem to a Parameter Optimization Problem

A standard optimal control problem in trajectory optimization is stated as follows: Minimize the performance index

$$J = \Phi(t_f, x_f) \tag{2.20}$$

subject to the n differential constraints

$$\dot{x} = f(t,x,u) \ , \tag{2.21}$$

the prescribed boundary conditions

$$\begin{aligned} &t_o = 0 \ , \quad x_o \equiv \text{given} \\ &\Psi(t_f, x_f) = 0 \ , \end{aligned} \tag{2.22}$$

the state variable inequality constraints

$$s_i(t,x) \leq 0 \ , \quad i = 1,\ldots,p \ , \tag{2.23}$$

and the control variable inequality constraints

$$c_j(t,x,u) \leq 0 \ , \quad j = 1,\ldots,q \ , \tag{2.24}$$

where x is a n-vector of state variables and u is a m-vector of control variables. This optimal control problem can be reduced to a suboptimal control problem which then can be solved using one of the current parameter optimization techniques.

First, the inequality constraints are considered. While the control variable inequality constraints may be handled locally, which will be described later, they are usually treated in the same way as the state variable inequality constraints. These are handled by imposing penalty functions on the performance index whenever the constraint is violated. Penalty functions may take different forms. Consider the following penalty functions which are based on the one given by Fletcher [7] :

$$P_k = \int_0^1 w_k \, e_k^2 \, d\tau \quad , \quad k = 1,\ldots,(p+q) \tag{2.25}$$

where the w_k are weighting constants and where the e_k are given by

$$\begin{aligned} e_k &= \min [- s_i , 0] \quad , \quad k = 1,\ldots,p \\ e_k &= \min [- c_j , 0] \quad , \quad k = (p+1),\ldots,(p+q) \end{aligned} \tag{2.26}$$

Here the s_i and c_j are the constraints as defined above. The weighting constants w_k are varied throughout the optimization process in order to aid convergence. If the (p+q) penalty functions (2.25) are differentiated, and P_k is called x_{n+k} , then

$$\dot{x}_{n+k} = w_k \, e_k^2 \quad , \quad k = 1,\ldots,(p+q) \tag{2.27}$$

where $P_{ko} = x_{n+k}(0) = 0$ and where $P_{kf} = x_{n+k}(t_f)$ is desired to be zero too (actually P_{kf} will be at least on the order of 10^{-6} to 10^{-8}). If the penalty functions x_{n+1} through x_{n+p+q} are now added to the state vector x and the resultant (n+p+q) - vector is called y, the original problem reduces to the following: Minimize the

performance index

$$J = \Phi_1(t_f, y_f)$$

subject to

$$\dot{y} = f_1(t, y, u) \tag{2.28}$$

with $t_o = 0$, $y_o \equiv$ given and

$$\Psi_1(t_f, y_f) = 0$$

where the functions Φ_1, f_1 and Ψ_1 are different from Φ, f and Ψ, respectively, because (p+q) states have been added.

The second step is to normalize the time. This introduces a new variable $\tau = t/t_f$ into the problem. The integration is now carried out with respect to τ, which allows the integration to cover the full range $0 \leq \tau \leq 1$ regardless of how the final time t_f is changed during the optimization process. Hence, Eqs. (2.28) become the following: Minimize the performance index

$$J = \Phi_1(t_f, y_f)$$

subject to

$$y' = \frac{d}{d\tau} y = t_f \, f_2(\tau, y, u, t_f) = g(\tau, y, u, t_f) \tag{2.29}$$

with $\tau_o = 0$, $y_o \equiv$ given , and

$$\tau_f = 1 \, , \; \Psi_1(t_f, y_f) = 0$$

Third, the control u is approximated with a known function of some unknown parameters $\alpha_1,\ldots,\alpha_l$, i.e., $u = u(\tau,\alpha_1,\ldots,\alpha_l)$, where the α_i are subject to optimization. Note that the α_i are m-vectors if u is a vector of m controls. If these parameters are spaced over the interval from $\tau_o = 0$ to $\tau_f = 1$ and represent the control at the times τ_i, then they are referred to as nodal points. The approximation of the actual control between the nodal points is found by interpolation, for example linear or higher-order interpolation such as the cubic spline. In the case of linear interpolation, control variable inequality constraints may be handled locally, as mentioned earlier. This means that the constraints are imposed on every nodal point. Throughout this report linear interpolation is assumed for simplicity. However, remarks will be made whenever higher-order interpolation would change results significantly.

If the $(1\cdot m)$ - vector $a = [\alpha_1,\ldots,\alpha_l]^T$ is defined, the equation for y' with $u = u(\tau,a)$ changes to

$$y' = g_1(\tau,y,a,t_f) \quad . \tag{2.30}$$

Integration of y' with $\tau_o = 0$ and $y_o \equiv$ given yields

$$y = y(\tau,a,t_f) \tag{2.31}$$

which, at the final point where $\tau_f = 1$, becomes

$$y_f = y(a,t_f) \tag{2.32}$$

Hence, the final states y_f are functions of $(1\cdot m + 1)$ parameters.

If this vector of (l•m + 1) parameters is called X , the original optimal control problem has been simplified to the following parameter optimization problem : Minimize the performance index

$$J = F(X) \tag{2.33}$$

subject to

$$C(X) = 0 \tag{2.34}$$

This parameter optimization problem is often referred to as the suboptimal control problem, because the function-space minimum is approximated by the solution to this parameter optimization problem. This is due to the approximation of the control. How well the actual solution is approximated will depend on the spacing and distribution of the nodal points over the time-interval as well as on the form of interpolation.

To formulate trajectory optimization problems a certain set-up procedure has to be followed. First, the adequate performance index is found form a careful analysis of the problem. To find the numerical value of the performance index at the final point, the differential equations $y' = g(\tau, y, a, t_f)$ have to be integrated. They consist of the n differential equations x', which are the equations of motion of the vehicle, and of the (p+q) differential equations for the penalty functions. To create the penalty functions, constraints have to be formulated. Possible control variable inequality constraints include constraints for the thrust, such as $T \leq T_{max}$, or for the lift-

coefficient, such as $C_{Lmin} \leq C_L \leq C_{Lmax}$. Such a double constraint may be converted to the standard form $c_j \leq 0$ in different ways. One possibility is given by

$$- (C_L - C_{Lmin})(C_{Lmax} - C_L) \leq 0 \qquad (2.35)$$

Possible state variable inequality constraints are also given directly by the specific problem and include constraints like $h \geq 0$ or $V \geq V_{stall}$.

To be able to integrate the differential equations y', initial conditions have to be given. These initial conditions as well as the final conditions that are needed for the optimization have to be stated in terms of the states. This is automatically done in methods that use the all Euler angles as states. Methods that use other states, such as inertial accelerations or quaternion elements, require the boundary conditions to be transformed from the Euler angle space to the respective state space. This may not always be trivial. How to obtain these boundary conditions is shown in the appropriate sections.

Choosing the nodal points, i.e. the parameters α_i, requires some thought. First a reasonable initial guess of the control has to be found, which means that the user should have a good idea what the solution might look like. Second, the number of nodal points has to be chosen, which involves a compromise. Many nodal points allow the control to be approximated better but, on the other hand, raise the

cost, i.e., the computer time needed by the optimization. Next, the form of interpolation has to be chosen, which not only influences the computation time but also depends on the parameter optimization method used. Spacing of the nodal points will then result from the chosen interpolation form.

SECTION III

EULER - ANGLE METHODS

1. The Inertial-Acceleration Method

The idea behind this method is, as previously mentioned, based on the fact that the two Euler angles that give the velocity vector orientation may be expressed in terms of the velocity vector components in some reference frame, for instance the local horizon system. Because the velocity V is given through $\dot{X}$, $\dot{Y}$ and $\dot{h}$, the three differential equations for V, χ and γ are replaced by the differential equations for $\dot{X}$, $\dot{Y}$ and $\dot{h}$. This should remove the singularity in the $\dot{\gamma}$ equation.

1.1. Derivation

If the equations for the aerodynamic forces, the thrust and the weight are inserted, the dynamic equation (2.1) takes the form

$$\bar{F} = m\bar{a} = (-D + T\cos\varepsilon\cos\nu)\hat{i}_w + (T\cos\varepsilon\sin\nu - Q)\hat{j}_w - (T\sin\varepsilon + L)\hat{k}_w + mg\,\hat{k}_h \qquad (3.1)$$

The accleration $\bar{a}$ is given by

$$\bar{a} = \frac{d\bar{V}}{dt}$$

and, with $\bar{V} = \frac{d}{dt}\overline{EO}$, becomes

$$\bar{a} = \frac{d^2}{dt^2}\overline{EO} = \frac{d^2}{dt^2}(X\hat{i}_h + Y\hat{j}_h + Z\hat{k}_h)$$

If the relationship $Z = -h + \text{const}$ is considered, and it is remembered that the local horizon system is defined to be parallel to the ground axes system at all times, the acceleration $\bar{a}$ can be expressed with inertial accelerations as

$$\bar{a} = \ddot{X}\hat{i}_h + \ddot{Y}\hat{j}_h - \ddot{h}\hat{k}_h \qquad (3.2)$$

The wind axes in Eqs. (3.1) are now expressed in terms of the horizontal axes using the direction cosine matrix (2.4), so that Eqs. (3.1) and (3.2) can be combined to yield three scalar equations for the inertial accelerations :

$$\begin{aligned}
m\ddot{X} &= (T\cos\varepsilon\cos\nu - D)\cos\gamma\cos\chi + (T\cos\varepsilon\sin\nu - Q)(\sin\mu\sin\gamma\cos\chi - \\
&\quad - \cos\mu\sin\chi) - (T\sin\varepsilon + L)(\cos\mu\sin\gamma\cos\chi + \sin\mu\sin\chi) \\
m\ddot{Y} &= (T\cos\varepsilon\cos\nu - D)\cos\gamma\sin\chi + (T\cos\varepsilon\sin\nu - Q)(\sin\mu\sin\gamma\sin\chi + \\
&\quad + \cos\mu\cos\chi) - (T\sin\varepsilon + L)(\cos\mu\sin\gamma\sin\chi - \sin\mu\cos\chi) \qquad (3.3) \\
m\ddot{h} &= (T\cos\varepsilon\cos\nu - D)\sin\gamma - (T\cos\varepsilon\sin\nu - Q)\sin\mu\cos\gamma + \\
&\quad + (T\sin\varepsilon + L)\cos\mu\cos\gamma - mg
\end{aligned}$$

In most cases these dynamical equations can be simplified with the assumptions that the aircraft sideslip angle σ is zero as well as the thrust sideslip angle ν. For symmetrical configurations this results in the aerodynamic side force Q being zero too.

The trigonometric functions of the velocity yaw angle χ and the velocity pitch angle γ are expressed through the velocity components $\dot{X}$, $\dot{Y}$ and $\dot{h}$ according to Figure 5.

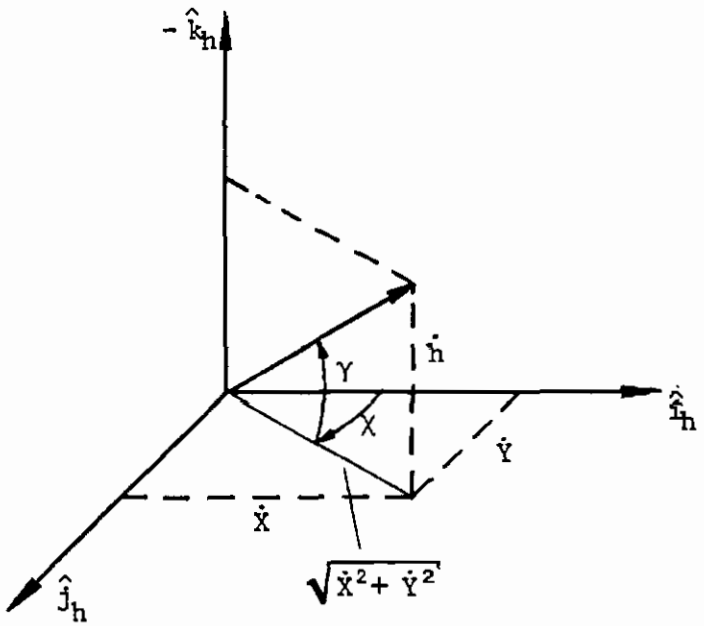

Figure 5 : Euler Angles and Velocity Components

Thus,

$$\sin\chi = \frac{\dot{Y}}{\sqrt{\dot{X}^2+\dot{Y}^2}} \quad , \quad \cos\chi = \frac{\dot{X}}{\sqrt{\dot{X}^2+\dot{Y}^2}}$$

$$\sin\gamma = \frac{\dot{h}}{V} \quad , \quad \cos\gamma = \frac{\sqrt{\dot{X}^2+\dot{Y}^2}}{V} \qquad (3.4)$$

These formulas are easily verified for the allowed values of χ and γ .

With the simplifications $\sigma = \nu = Q = 0$ and the conversion formulas (3.4), the second-order differential equations (3.3) become

$$
\begin{aligned}
m\ddot{X} &= (T\cos\varepsilon - D)\frac{\dot{X}}{V} - (T\sin\varepsilon + L)\left(\cos\mu\,\frac{\dot{h}}{V}\,\frac{\dot{X}}{\sqrt{\dot{X}^2+\dot{Y}^2}} + \sin\mu\,\frac{\dot{Y}}{\sqrt{\dot{X}^2+\dot{Y}^2}}\right)\\
m\ddot{Y} &= (T\cos\varepsilon - D)\frac{\dot{Y}}{V} - (T\sin\varepsilon + L)\left(\cos\mu\,\frac{\dot{h}}{V}\,\frac{\dot{Y}}{\sqrt{\dot{X}^2+\dot{Y}^2}} - \sin\mu\,\frac{\dot{X}}{\sqrt{\dot{X}^2+\dot{Y}^2}}\right)\\
m\ddot{h} &= (T\cos\varepsilon - D)\frac{\dot{h}}{V} + (T\sin\varepsilon + L)\cos\mu\,\frac{\sqrt{\dot{X}^2+\dot{Y}^2}}{V} - mg
\end{aligned}
\qquad (3.5)
$$

where $V = \sqrt{\dot{X}^2+\dot{Y}^2+\dot{h}^2}$. This set of second-order differential equations can be integrated numerically, using for instance one of the Runge-Kutta algorithms, after reducing it to a set of first-order differential equations and adding the mass equation $\dot{m} = -\beta$ to it. If $X_1 = X$, $X_2 = Y$, $X_3 = h$, $X_4 = \dot{X}$, $X_5 = \dot{Y}$, $X_6 = \dot{h}$ and $X_7 = m$, the equations of motion are as follows :

$$
\begin{aligned}
\dot{X}_1 &= X_4\\
\dot{X}_2 &= X_5\\
\dot{X}_3 &= X_6\\
\dot{X}_4 &= \frac{1}{X_7}\left\{(T\cos\varepsilon - D)\frac{X_4}{V} - (T\sin\varepsilon + L)\left(\cos\mu\,\frac{X_6}{V}\,\frac{X_4}{\sqrt{X_4^2+X_5^2}} + \sin\mu\,\frac{X_5}{\sqrt{X_4^2+X_5^2}}\right)\right\}\\
\dot{X}_5 &= \frac{1}{X_7}\left\{(T\cos\varepsilon - D)\frac{X_5}{V} - (T\sin\varepsilon + L)\left(\cos\mu\,\frac{X_6}{V}\,\frac{X_5}{\sqrt{X_4^2+X_5^2}} - \sin\mu\,\frac{X_4}{\sqrt{X_4^2+X_5^2}}\right)\right\}\\
\dot{X}_6 &= \frac{1}{X_7}\left\{(T\cos\varepsilon - D)\frac{X_6}{V} + (T\sin\varepsilon + L)\cos\mu\,\frac{\sqrt{X_4^2+X_5^2}}{V}\right\} - g\\
\dot{X}_7 &= -\beta
\end{aligned}
\qquad (3.6)
$$

where $V = \sqrt{X_4^2 + X_5^2 + X_6^2}$. Analogous to the equations of motion of Section II.2., this set of equations has μ , α and π as controls if the engine is fixed to the aircraft.

To be able to integrate the above equations, initial conditions for X_1 through X_7 are needed. While X_{1o} and X_{2o} are usually chosen to be zero, X_{3o} is the initial altitude h_o. X_{4o} through X_{6o} are computed from the initial values of the velocity V_o, the flight path angle γ_o and the velocity yaw angle χ_o according to the kinematic equations (2.6). Thus Eqs. (3.6) are integrated subject to the initial conditions :

$$
\begin{aligned}
&X_{1o} = 0 \quad , \quad X_{2o} = 0 \quad , \quad X_{3o} = h_o \\
&X_{4o} = V_o \cos\gamma_o \cos\chi_o \\
&X_{5o} = V_o \cos\gamma_o \sin\chi_o \\
&X_{6o} = V_o \sin\gamma_o \\
&X_{7o} = m_o
\end{aligned}
\tag{3.7}
$$

The final conditions will usually be stated in terms of V, the final aircraft attitude and/or the final altitude h. To yield a feasible set of final conditions for optimization, Eqs. (3.7) are used and combined in such a way that the variables with unspecified final values vanish. These equations form then the set of final conditions which may be added to the performance index as a penalty function as has been shown in Section II.3.

1.2. Discussion

Examination of the equations of motion as given by Eqs. (3.6) discloses problems for X_4 and X_5 being zero at the same time. Since $X_4 = \dot{X}$ and $X_5 = \dot{Y}$, this happens when the aircraft is flying straight up or down. Comparison with Eqs. (3.4) shows that these terms, which become undefined for $\dot{X} = \dot{Y} = 0$, are exactly the expressions for $\sin\chi$ and $\cos\chi$. Since the heading angle is not defined when $\gamma = +/- 90$ deg, this result makes sense. It is noted, however, that it is practically impossible to achieve $\dot{X}$ and $\dot{Y}$ equal to zero at exactly the same time during numerical integration, unless the trajectory is started out at the vertical position. Because the control can only be changed in finite steps, $\dot{X}$ and $\dot{Y}$ will stay nonzero even for third-class trajectories, as long as the trajectory is not started out in the vertical position.

A different problem arises, though. As discussed in Section II.1, the bank angle and the velocity yaw angle have simultaneously a singularity during second- or third-class trajectories. The singularity in χ will be determined by $\dot{X}$ and $\dot{Y}$, namely when $\dot{X}$ and $\dot{Y}$ go through zero at the same time. Unless the integration stepsize is varied so as to integrate right up to that point, $\dot{X}$ and $\dot{Y}$ almost certainly will go through zero inside an integration step. Since the bank angle is a control, which is only changed at predetermined times t_k by the optimization algorithm, a conflict arises. What happens if μ is not changed at exactly the time where $\dot{X}$

and $\dot{Y}$ go through zero is shown in Figs. 6 and 7. Simulated is the Split-S maneuver, started for simplicity in the $\chi = 0$ direction, so that $\dot{Y} = 0$ for the whole trajectory. From Figure 6 it is seen that γ stays at a fixed value after it is supposed to hit $\gamma = -90$ deg. Whether or not the vertical line has been crossed will depend on the signs of $\dot{X}$ and $\dot{Y}$ after that point. Why γ stays fixed is explained by Fig. 7, which shows $\dot{X}$ and $\ddot{X}$ every time the integration routine (classical RK4) evaluates the differential equations, along with the equations for $\dot{X}$ and $\ddot{X}$. These are rewritten here as follows:

$$\dot{X} = X_4$$

$$\ddot{X} = \dot{X}_4 = \frac{1}{X_7}\left\{(T\cos\varepsilon - D)\frac{X_4}{V} - (T\sin\varepsilon + L)\cos\mu\frac{X_6}{V}\frac{X_4}{\sqrt{X_4^2}}\right\}$$

where $\dot{X}_5 = \dot{Y} = 0$ has been used. Note that $\dot{X}$ stays positive until the negative $\ddot{X}$ drives $\dot{X}$ through zero to a negative value (point 1 in Fig. 7). Since $\cos\mu$ is not changed and because X_4/V is small, the sign change in $\dot{X}$ changes the sign of $\ddot{X}$ (point 2). This drives $\dot{X}$ back to a positive value (point 3), which in turn changes $\ddot{X}$ back to a negative value the next time the differential equations are evaluated. This goes back and forth, and the position of the aircraft at the end of the integration step will be determined by the value of $\dot{X}$ as computed by the integrator RK4. This uncertainty in whether χ will change or not makes it hard to check numerically if $\gamma = +/- 90$ deg has actually been achieved.

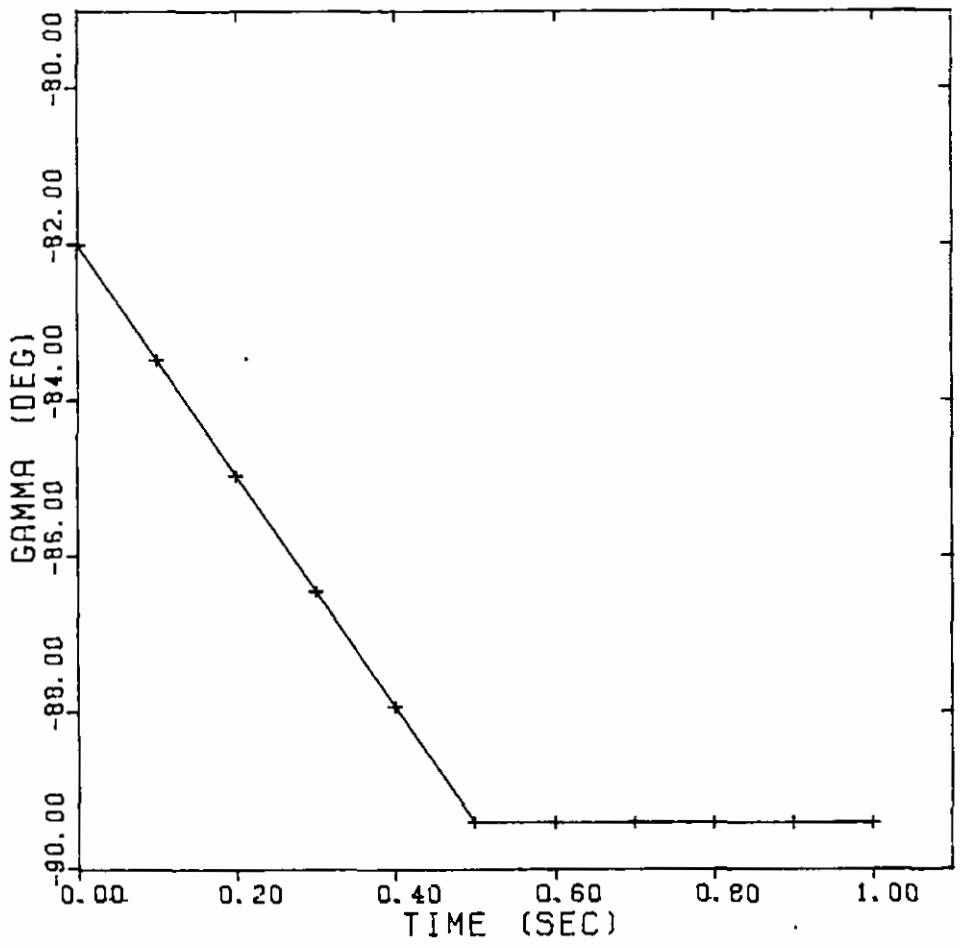

Figure 6 : γ versus Time for an Attempted Split-S with the Unmodified Inertial-Acceleration Method

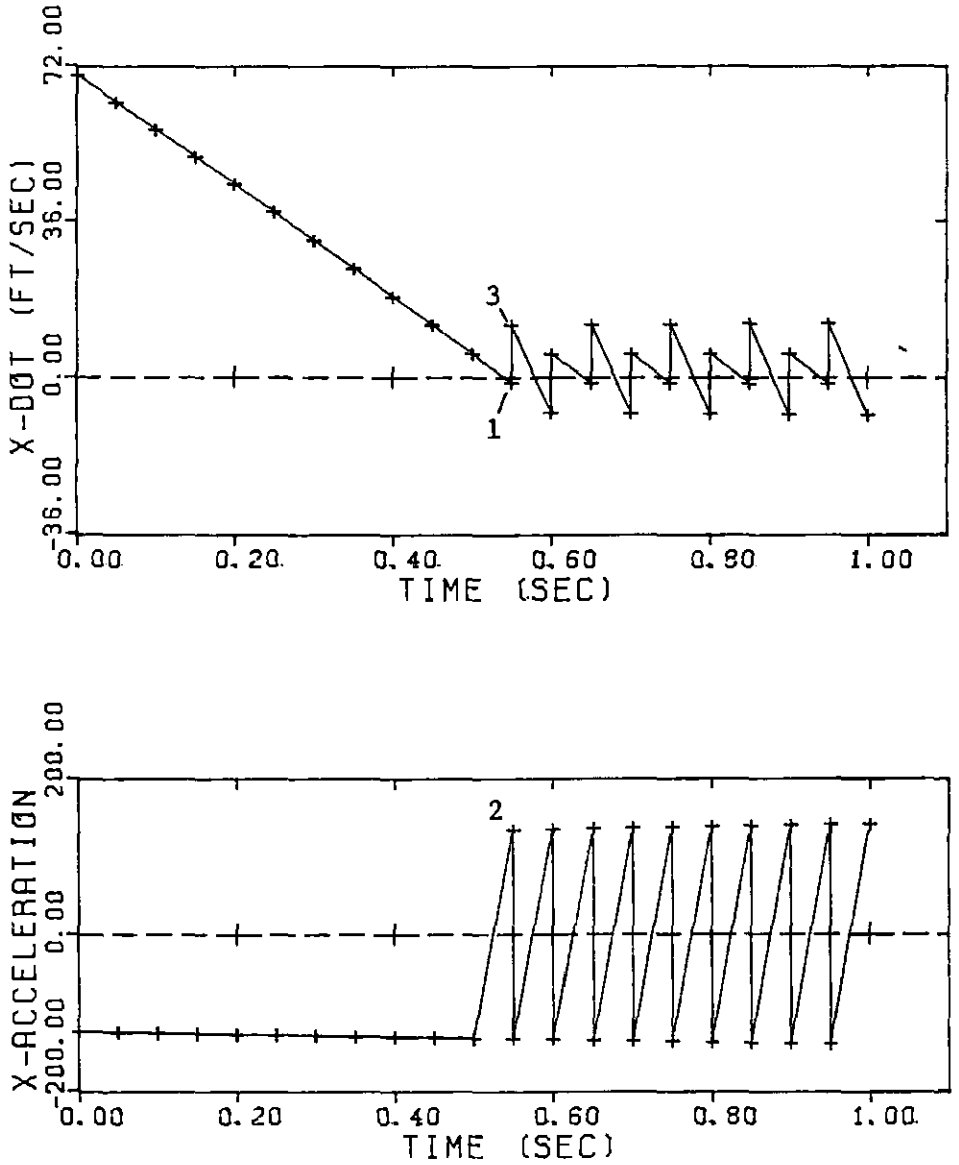

Figure 7 : $\dot{X}$ and $\ddot{X}$ versus Time for the Split-S of Figure 6

To solve this problem, it is necessary to integrate with decreasing stepsizes up to the vertical position, after predicting when this point is likely to occur. Such an estimation will be fairly easy for most second-class trajectories such as the Split-S where γ changes almost linearly. A simple algorithm may look as follows :

1. Compute the last increase in γ : $\Delta\gamma_k = |\gamma_k - \gamma_{k-1}|$

2. If $|\gamma_k| + \Delta\gamma_k \geq \pi/2$, choose as the new stepsize

$$\Delta t_{k+1} = \text{Const} \frac{\pi/2 - |\gamma_k|}{\Delta\gamma_k} \Delta t_k$$

The constant is chosen between 0.5 and 0.9 , depending on the expected trajectory, so as to assure that γ = +/- 90 deg is not crossed and the integration errors do not pile up too much due to a slow convergence of γ . The vertical attitude is then achieved within a certain border once the stepsize falls below a given limit.

At this point the program will ask for a new μ , which ought to be the old μ plus or minus 180 deg. Since the vertical position is not achieved completely, $\dot{X}$ and $\dot{Y}$ have not gone through zero but are close to zero. To pass through the vertical position, $\dot{X}$ and $\dot{Y}$ are driven through zero at the same time the new bank angle is input. This is done by simply changing their signs (this compares with flipping the heading angle around). Not changing these two signs makes the aircraft come out with the same heading angle it had before entering the vertical position, but because μ is changed, a half roll is performed at the vertical position. If the sign of only one

velocity component is changed, a direction change between 0 deg and 180 deg is made, depending on the last heading angle and the velocity component being changed.

The inertial-acceleration method will work fine in simple interactive programs, where the operator specifies the initial values and the control history up to γ = +/- 90 deg. When the program then asks for a new μ at the vertical position, the new μ is input and the program continues until some final criteria are met. That new μ may also be specified automatically when γ = +/- 90 deg is reached since it is known that $\mu_{new} = \mu_{old}$ +/- 180 deg.

In parameter optimization methods where the control history is given by interpolation between nodal points, the inertial-acceleration method seems to create problems at first. If the singularity in μ occurs between the nodal points at times t_k and t_{k+1}, the actual jump in μ will be approximated by interpolation, where the change of μ will depend on the spacing of the nodal points. The number of nodal

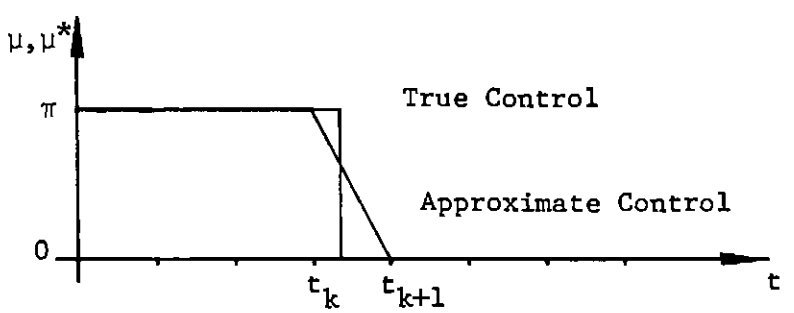

Figure 8 : True Control and Control Approximation for the Split-S

points, however, should be kept as low as possible, as mentioned in Section II.3. The true control history for the Split-S maneuver and the approximation used in the optimization are shown in Figure 8 .

The idea might arise that such a control would simply lead the trajectory around the exact vertical position into the right post-vertical direction. Some computer runs have shown this to be wrong. Figures 9 through 11 show the time interval from t_k to t_{k+1} for different initial conditions. It is seen that the trajectory might break away in any direction, depending on the combination of lift-coefficient and the starting point of the rolling maneuver. The closer $\gamma = -90$ deg is approached, the higher the associated change in the heading angle (see Fig.11). Because the control history changes after each iteration of the optimization algorithm, it will not be known exactly when $\gamma = 90$ deg will occur, and it seems almost impossible to find the correct control that leads around the vertical position and still ends up in the right direction (as in Figure 10). It is also very difficult and costly for the optimization algorithm to find the jump in μ if it occurs between the wrong nodal points in the initial guess.

The problems associated with the use of the inertial-acceleration method for parameter optimization are easily solved using a dummy control for the optimization and another control for the integration of the equations of motion. It should be remembered that the vertical position is predicted in the inertial-acceleration

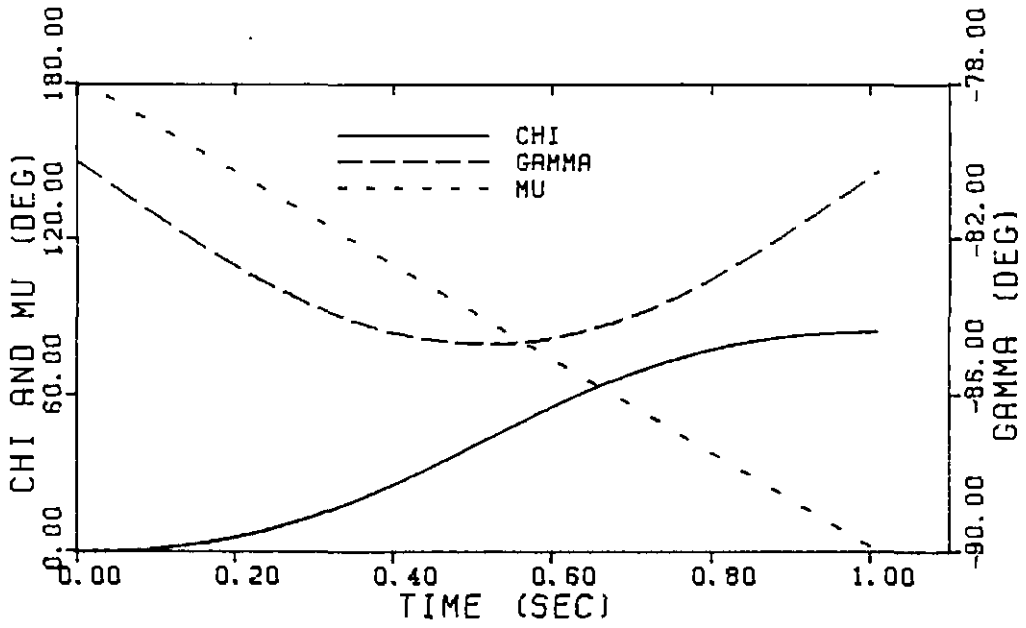

Figure 9 : Linear Change in μ, Starting at γ = - 80 deg

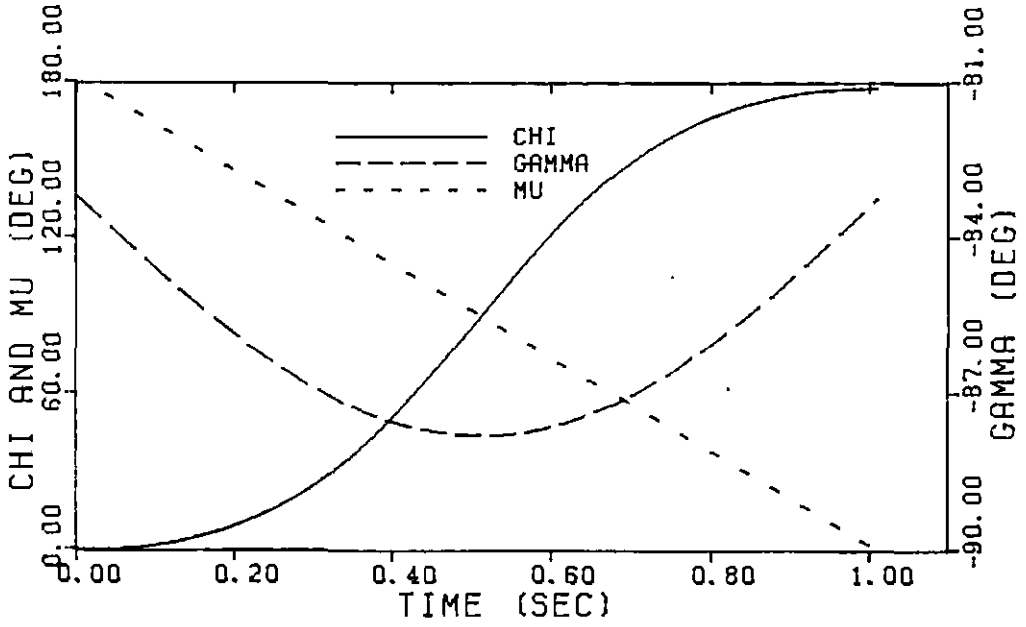

Figure 10 : Linear Change in μ , Starting at γ = - 83.2 deg

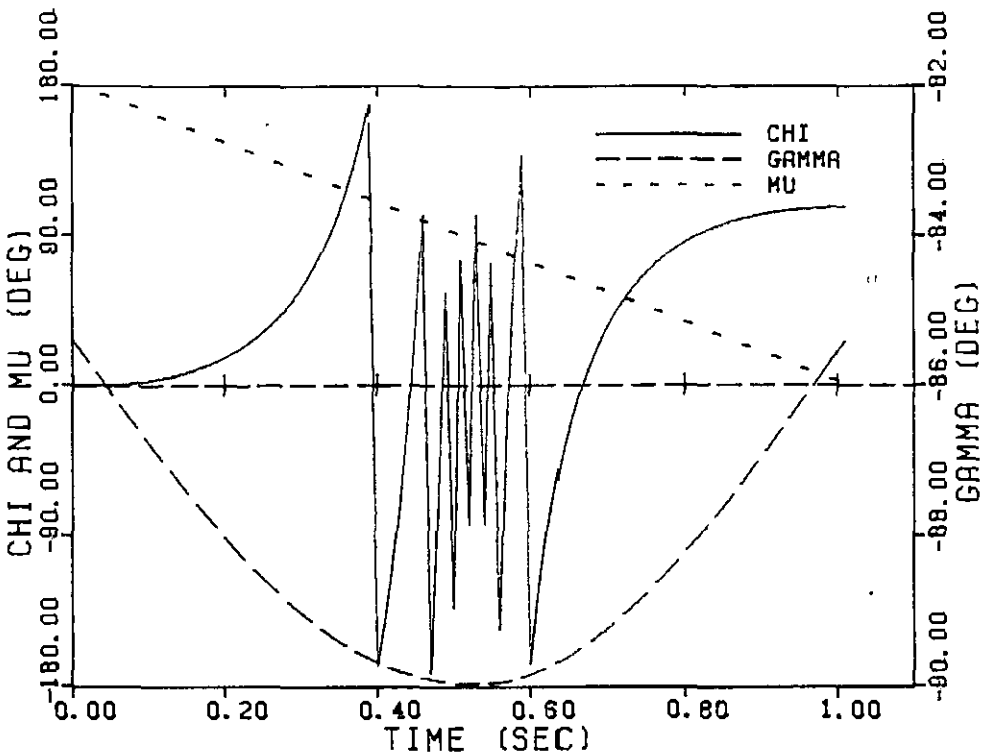

Figure 11 : Linear Change in μ , Starting at γ = - 85.4 deg

method, and the trajectory is integrated up to that point. The bank angle is then changed by plus or minus 180 deg, which can be done by the integration-leading subroutine. It is easy to simply add or substract 180 deg to μ at all subsequent nodal points while holding at the vertical position. The optimization is then carried out with respect to some continuous dummy control, say μ^*. The real control μ which is relevant for the integration agrees with that μ^* up until $\gamma = 90$ deg is reached first. From then on μ differs from μ^* by 180 deg until the vertical position is encountered again. This may be illustrated by an example. If an aircraft starts with a steeply-banked right turn, continues rolling into the Split-S maneuver and then rolls out into a level left turn, the bank angle history μ and the dummy control history μ^* might look as illustrated in Figure 12. Note that the jump in μ could now occur anywhere between two nodal points, that is when the vertical position is achieved.

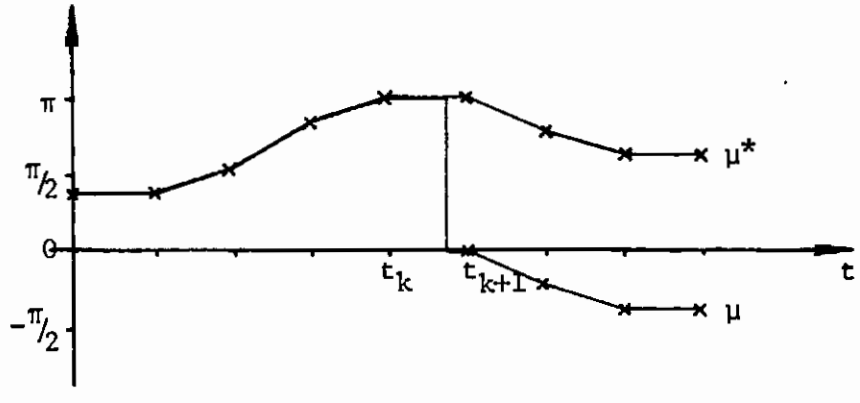

Figure 12 : The Dummy Control μ^*

This shows that the inertial-acceleration method will perform well for parameter optimization of second-class trajectories. Third-class trajectories cannot be integrated in the strict mathematical sense but will cause no problems unless started out in the vertical position. Only in that case would the horizontal speed components be exactly zero and make some terms in the equations of motion undefined.

2. The Two - System Method

Since the singularities in the Euler angles appear when one angle, namely γ, hits +/- 90 deg, it might be possible to switch to some other set of equations when approaching γ = +/- 90 deg. That set of equations of motion, in the following called set 2, would be derived on the basis of a vertical reference system in a way similar to the derivation of the usual equations. Therefore, it would have its singularities for horizontal flight, and by switching back to set 1, the set based on the horizon axes system, long before horizontal flight is achieved, no singularities would appear. Analogous to the Euler-angle sequence used in set 1, set 2 is derived using a yaw-pitch-roll Euler-angle sequence, although any other sequence such as roll-pitch-yaw could be used as long as the necessary conversion formulas from set 1 to set 2 and vice versa are given. This is mentioned because specific Euler-angle sequences might have advantages for certain trajectories, as will be seen later.

The Euler angles based on the vertical reference system will be called ψ for the velocity yaw angle, θ for the velocity pitch angle, and ϕ for the velocity roll angle. These angles are measured from the vertical reference frame, which has its x-axis pointing along the z-axis of the horizontal system ("downwards"), its y-axis coinciding with the y-axis of the horizontal system, and its z-axis so as to complete the right-hand set (see Figure 13). Thus, the reference attitude of the aircraft is a vertical dive, and the

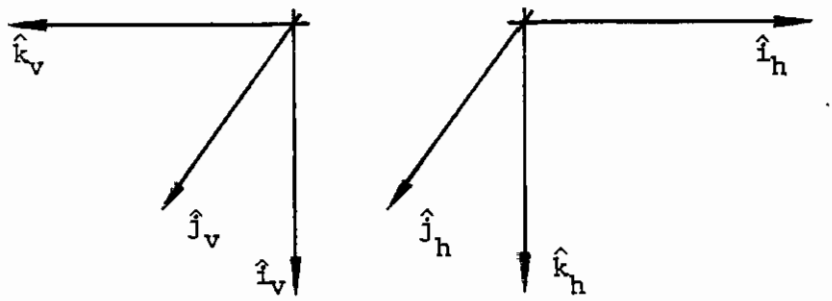

(a) (b)

Figure 13 : (a) - The Vertical Reference System (for Set 2)

(b) - The Horizontal Reference System (for Set 1)

velocity pitch angle θ , for instance, is measured from the vertical $\hat{i}_v$-axis. The body-axes system stays the same for set 2 as it is for set 1, which means that the sideslip angle σ and the angle of attack α are defined as before, as well as the thrust sideslip angle ν and the thrust angle of attack ε .

Since the velocity roll rate, p_w, the velocity pitch rate, q_w, and the velocity yaw rate, r_w, are measured in the wind axes system, they are independent of the reference system used and, thus, stay the same as before. They are related to the angular velocity $\bar{\omega}$ through Eq. (2.12) :

$$\bar{\omega} = p_w\hat{i}_w + q_w\hat{j}_w + r_w\hat{k}_w$$

2.1. Derivation

Because the same yaw-pitch-roll rotation sequence is used, the same direction cosine matrix is valid for the rotation of the vertical reference system into the wind axes system. Replacing the corresponding unit-vectors and Euler angles in Eqs. (2.4) leads to

$$\begin{bmatrix} \hat{i}_w \\ \hat{j}_w \\ \hat{k}_w \end{bmatrix} = \begin{bmatrix} \cos\theta\cos\psi & \cos\theta\sin\psi & -\sin\theta \\ \sin\phi\sin\theta\cos\psi - \cos\phi\sin\psi & \sin\phi\sin\theta\sin\psi + \cos\phi\cos\psi & \sin\phi\cos\theta \\ \cos\phi\sin\theta\cos\psi + \sin\phi\sin\psi & \cos\phi\sin\theta\sin\psi - \sin\phi\cos\psi & \cos\phi\cos\theta \end{bmatrix} \begin{bmatrix} \hat{i}_v \\ \hat{j}_v \\ \hat{k}_v \end{bmatrix} \tag{3.8}$$

Again, the inverse of the direction cosine matrix is given by its transpose.

The actual derivation of the equations of motion for the vertical reference system is now very similar to the one presented in Section II.2, where use of the following identities is made:

$$\begin{aligned} \hat{i}_h &= -\hat{k}_v \\ \hat{j}_h &= \hat{j}_v \\ \hat{k}_h &= \hat{i}_v \ . \end{aligned} \tag{3.9}$$

These identities are easily verified using Figure 13. Thus, Eq. (2.3) converts to

$$V\hat{i}_w = -\dot{X}\hat{k}_v + \dot{Y}\hat{j}_v - h\dot{\hat{i}}_v \tag{3.10}$$

which leads with Eqs. (3.8) to the three kinematic relationships

$$\begin{aligned} \dot{X} &= V \sin\theta \\ \dot{Y} &= V \cos\theta \sin\psi \\ \dot{h} &= -V \cos\theta \cos\psi \end{aligned} \tag{3.11}$$

The dynamic equation is given by

$$\bar{T} + \bar{A} + m\bar{g} = m\bar{a} = m \frac{d}{dt} \bar{V}$$

where

$$\bar{T} = T (\cos\varepsilon \cos\nu \hat{i}_w + \cos\varepsilon \sin\nu \hat{j}_w - \sin\varepsilon \hat{k}_w)$$

$$\bar{A} = - D\hat{i}_w - Q\hat{j}_w - L\hat{k}_w$$

$$\frac{d}{dt} \bar{V} = \dot{V}\hat{i}_w + V r_w \hat{j}_w - V q_w \hat{k}_w \ ,$$

but, because $\hat{k}_h = \hat{i}_v$,

$$\bar{g} = g\hat{i}_v \ . \tag{3.12}$$

After expressing $\hat{i}_v$ in terms of $\hat{i}_w$, $\hat{j}_w$ and $\hat{k}_w$ using the transpose of the direction cosine matrix (3.8), this results in the three scalar equations

$$\begin{aligned} m\dot{V} &= T \cos\varepsilon \cos\nu - D + mg \cos\theta \cos\psi \\ mVr_w &= T \cos\varepsilon \sin\nu - Q + mg (\sin\phi \sin\theta \cos\psi - \cos\phi \sin\psi) \\ mVq_w &= T \sin\nu + L - mg (\cos\phi \sin\theta \cos\psi + \sin\phi \sin\psi) \ . \end{aligned} \tag{3.13}$$

Again, because the rotation sequence has not changed, p_w, q_w and r_w

are related to the Euler angle rates $\dot{\psi}$, $\dot{\theta}$ and $\dot{\phi}$ according to Eqs. (2.15) after substituting the corresponding angles :

$$\begin{aligned} p_w &= \dot{\phi} - \dot{\psi}\sin\theta \\ q_w &= \dot{\theta}\cos\phi + \dot{\psi}\sin\phi\cos\theta \\ r_w &= -\dot{\theta}\sin\phi + \dot{\psi}\cos\phi\cos\theta \end{aligned} \tag{3.14}$$

Substituting Eqs. (3.14) into Eqs. (3.13) and solving for ψ and θ leads to the dynamical relationships which, along with the mass equation and the kinematic equations (3.11), form the following set of differential equations :

$$\begin{aligned} \dot{X} &= V\sin\theta \\ \dot{Y} &= V\cos\theta\sin\psi \\ \dot{h} &= -V\cos\theta\cos\psi \\ m\dot{V} &= T\cos\varepsilon\cos\nu - D + mg\cos\theta\cos\psi \\ mV\dot{\psi} &= \frac{1}{\cos\theta}\left\{(T\cos\varepsilon\sin\nu - Q)\cos\phi + (T\sin\varepsilon + L)\sin\phi - mg\sin\psi\right\} \\ mV\dot{\theta} &= (T\sin\varepsilon + L)\cos\phi - (T\cos\varepsilon\sin\nu - Q)\sin\phi - mg\sin\theta\cos\psi \\ \dot{m} &= -\beta \end{aligned} \tag{3.15}$$

With the same assumptions as in Section II.2, namely fixed engine and $\sigma = \nu = Q = 0$, this set of differential equations has three mathematical degrees of freedom. The three controls will usually be the bank angle ϕ, the power setting π and the angle of attack α, or the lift coefficient C_L, respectively.

To be able to switch from one set of differential equations to the other, the relationships between the Euler angles χ , γ and μ of

the horizontal reference system and the Euler angles ψ , θ and ϕ of the vertical reference system are needed. Since every aircraft attitude could be achieved from either reference system by rotating that reference system through the appropriate Euler angles, the expression for the wind axes unit vectors as given in Eqs. (2.4) and Eqs. (3.8) can be equated. For $\hat{i}_w$ this leads to

$$\hat{i}_h \cos\gamma \cos\chi + \hat{j}_h \cos\gamma \sin\chi - \hat{k}_h \sin\gamma = \\ = \hat{i}_v \cos\theta \cos\psi + \hat{j}_v \cos\theta \sin\psi - \hat{k}_v \sin\theta$$

Remembering that $\hat{i}_v = \hat{k}_h$, $\hat{j}_v = \hat{j}_h$ and $\hat{k}_v = - \hat{i}_h$ yields three identities. Applying the same procedure to the equations for $\hat{j}_w$ and $\hat{k}_w$ results in a total of nine identities between the two sets of Euler angles :

$$\cos\theta \cos\psi = - \sin\gamma \tag{3.16}$$

$$\cos\theta \sin\psi = \cos\gamma \sin\chi \tag{3.17}$$

$$\sin\theta = \cos\gamma \cos\chi \tag{3.18}$$

$$\sin\phi \sin\theta \cos\psi - \cos\phi \sin\psi = \sin\mu \cos\gamma \tag{3.19}$$

$$\sin\phi \sin\theta \sin\psi + \cos\phi \cos\psi = \sin\mu \sin\gamma \sin\chi + \cos\mu \cos\chi \tag{3.20}$$

$$\sin\phi \cos\theta = - \sin\mu \sin\gamma \cos\chi + \cos\mu \sin\chi \tag{3.21}$$

$$\cos\phi \sin\theta \cos\psi + \sin\phi \sin\psi = \cos\mu \cos\gamma \tag{3.22}$$

$$\cos\phi \sin\theta \sin\psi - \sin\phi \cos\psi = \cos\mu \sin\gamma \sin\chi - \sin\mu \cos\chi \tag{3.23}$$

$$\cos\phi \cos\theta = - \cos\mu \sin\gamma \cos\chi - \sin\mu \sin\chi \tag{3.24}$$

The same idea holds for the angular velocity of the wind-axes system, $\bar{\omega}$. Equating Eqs. (2.15) and Eqs. (3.14) gives the following

three relationships :

$$\dot{\phi} - \dot{\psi}\sin\theta = \dot{\mu} - \dot{\chi}\sin\gamma \tag{3.25}$$

$$\dot{\theta}\cos\phi + \dot{\psi}\sin\phi\cos\theta = \dot{\gamma}\cos\mu + \dot{\chi}\sin\mu\cos\gamma \tag{3.26}$$

$$-\dot{\theta}\sin\phi + \dot{\psi}\cos\phi\cos\theta = -\dot{\gamma}\sin\mu + \dot{\chi}\cos\mu\cos\gamma \; . \tag{3.27}$$

The velocity yaw angle as measured from the vertical reference system is now given by Eqs. (3.16) and (3.17) as

$$\psi = \arctan\frac{\cos\gamma\sin\chi}{-\sin\gamma} \; . \tag{3.28}$$

This will yield the full range of ψ when using the computer library function ATAN2 , except for $\chi = 0$ deg and $\gamma = 0$ deg or $\chi = 180$ deg and $\gamma = 180$ deg, at which points the set 2 equations are not used anyway. The velocity pitch angle θ is simply given by Eq. (3.18), since it is resticted to +/- 90 deg. Therefore,

$$\theta = \arcsin(\cos\gamma\cos\chi) \tag{3.29}$$

Finally, Eq. (3.21) is divided by Eq. (3.24) to yield the velocity roll angle

$$\phi = \arctan\frac{-\sin\mu\sin\gamma\cos\chi + \cos\mu\sin\chi}{-\cos\mu\sin\gamma\cos\chi - \sin\mu\sin\chi} \tag{3.30}$$

which again will give the full range of the bank angle, except for $\chi = 0$ deg and $\gamma = 0$ deg, or $\chi = 180$ deg and $\gamma = 180$ deg respectively. Note that signs should not be cancelled in Eqs. (3.28) or (3.30) if ATAN2 is to give the correct angle.

When switching back to set 1, the set 1 Euler angles have to be computed from the set 2 Euler angles. The necessary equations are found as above and are given by

$$\chi = \arctan \frac{\sin\psi \cos\theta}{\sin\theta} \tag{3.31}$$

$$\gamma = - \arcsin (\cos\psi \cos\theta) \tag{3.32}$$

$$\mu = \arctan \frac{\sin\phi \sin\theta \cos\psi - \cos\phi \sin\psi}{\cos\phi \sin\theta \cos\psi + \sin\phi \sin\psi} \tag{3.33}$$

2.2 Discussion

The two-system method uses two sets of equations of motion, where the set 1 equations are based on a local horizon system, and where the set 2 equations are based on a vertical reference system. Both sets of differential equations use the power setting, the angle of attack and the velocity bank angle, as measured from the corresponding reference system, as controls. Since the controls π and α are independent of the reference system used, they are the same for the set 1 equations as for the set 2 equations, thus being continuous when switching from one system to the other. The bank angle, however, is based on the reference system and, therefore, is different when measured from the local horizon system than when measured form the vertical reference system. Figure 14 shows the set 1 and the set 2 Euler angles for a loop that is started upside down like a Split-S. It shows that switching from one set of equations to the other set of equations generally results in a discontinuity in the bank angle, i.e. control.

Three possibilities exist to handle this discontinuity. First, the discontinuity can be removed by retaining the bank angle of system 1, i.e. μ , as control throughout the whole trajectory. In this case ϕ , the bank angle of set 2, has to be computed from μ as long as the set 2 equations are used. Because χ and γ are no longer available, ϕ may be found from μ , ψ and θ after replacing the expressions for χ and γ in Eq. (3.30) using Eqs. (3.16) through (3.18). This leads to

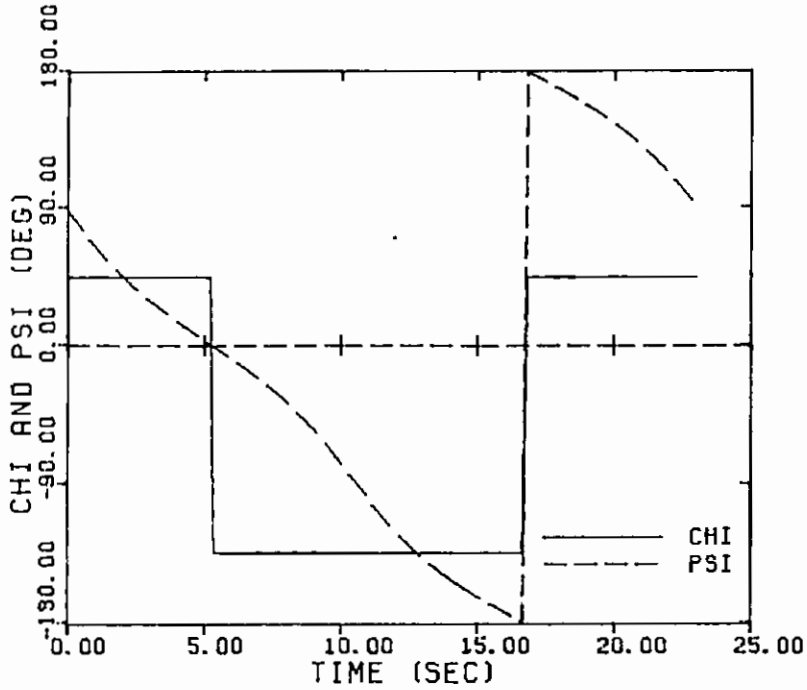

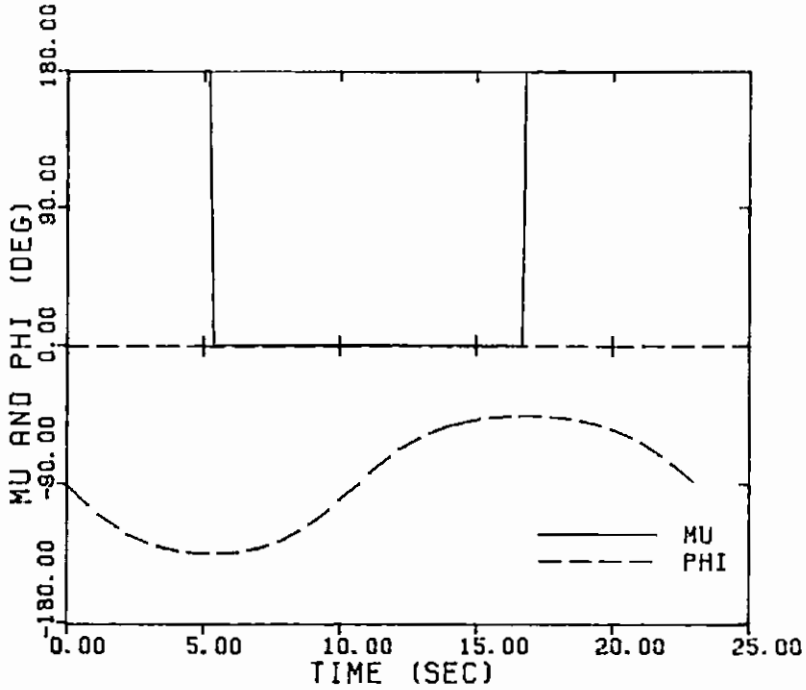

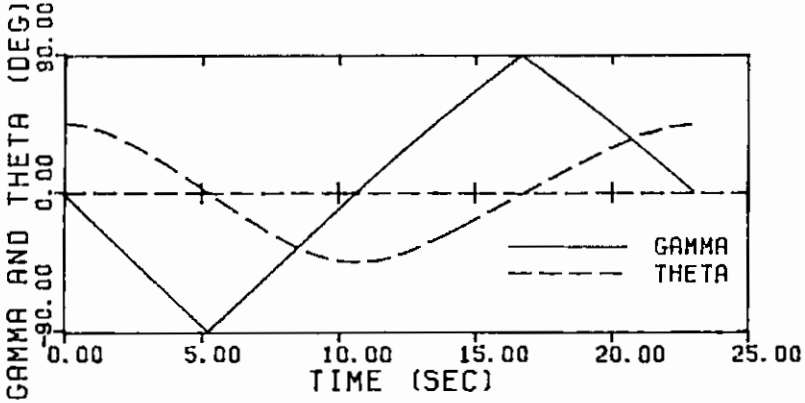

Figure 14 :

Set 1 and Set 2 Euler Angles for

a Loop (Started as a Split-S)

the following equation:

$$\phi = \arctan \frac{\sin\mu \cos\psi \sin\theta + \cos\mu \sin\psi}{\cos\mu \cos\psi \sin\theta - \sin\mu \sin\psi} \tag{3.34}$$

This updating formula is used to compute ϕ every time the differential equations are evaluated. Since μ has to be input as control, the integration has to be stopped at the vertical position where μ is changed. The optimization is now carried out in a way similar to the one presented for the inertial-acceleration method, i.e. by using a dummy control.

The second way of handling the switching discontinuity in the bank angle employes a roll-pitch-yaw rotation sequence for the set 2 equations. It should be understood that every trajectory behaves like the Split-S or the Immelmann maneuver near the vertical position as long as the sideslip angles are set to zero. This is true because the vertical position can only be assumed if the bank angle μ is either 0 deg or +/- 180 deg. If a roll-pitch-yaw rotation sequence is chosen for the vertical reference system, it turns out that the velocity roll angle stays constant throughout a Split-S or a loop and corresponds to the heading angle χ as measured from the local horizon system. The equations of motion for such a rotation sequence are derived in Appendix A along with the necessary Euler angle conversion formulas. It turns out that this system allows integration across the vertical line without having to stop the integration procedure, under the assumption that the roll-rate p_w can be set to zero during the time

this system is used. Third-class trajectories can be integrated as long as they include no vertical rolls, i.e. only straight, vertical climbs or dives. This roll-pitch-yaw two-system method will give the right control μ when switching back to the set 1 equations. At this point the integration should be stopped, and the dummy control μ^*, used in the parameter optimization, should be changed by +/- 180 deg to yield the correct values for μ at the nodal points. This dummy control is also necessary for the first derived yaw-pitch-roll two-system method, the difference being that the nodal points are updated while stopping at γ = +/-90 deg.

The third possibility of handling the switching-discontinuity in the control involves more effort on the user's part, since both bank angles are kept as control. As long as the trajectory is not close to the vertical position μ is used as control, where μ is found through interpolation from the nodal points. When a certain predetermined flight path angle close to γ = +/- 90 deg is reached, the integration is stopped. The integration leading subroutine goes back in time to the last nodal point. Now the next set 2 nodal points can only be computed from the corresponding set 1 nodal points if χ and γ for these points are known besides μ. Otherwise they have to be guessed. Now the integration is continued with the set 2 equations of motion. When the aircraft is well clear of the vertical position, the integration is switched back to the set 1 equations. This is done as above after going back in time to the last nodal point. It is seen that this procedure is quite troublesome. It is only useful if the

user has a very good idea how the solution to his trajectory otimization problem has to look like. The user should know where the switching to the set 2 equations takes place, and he should be able to provide initial guesses for the set 2 nodal points. Hence, this method is very restrictive. It cannot be used for problems where it is not known if and where the vertical position is assumed, unless the user takes the risk of high computation costs. These result when the set 2 nodal points are not provided initially and have to be found from scratch in the optimization procedure. The only advantage of this method is that it allows even third-class trajectories that include rolls at the vertical position to be optimized. This results from ϕ being the control in the vicinity of that point.

3. A Trivial Solution for Flight in the Vertical Plane

For flight in the vertical plane the heading angle χ and the bank angle μ can only have values of 0 deg or 180 deg. The positive X direction will be characterized by $\chi = 0$ deg, whereas the negative X direction will be assumed for $\chi = +/- 180$ deg. The idea of this method is to remove the +/- 90 deg constraint on γ, thus covering the negative X direction with flight path angles of more than 90 deg, while at the same time leaving χ equal to zero. It appears that this method has been previously used [4].

Since the differential equation for χ is not needed anymore, the usual set of equations of motion can be integrated for all flight path angles. These equations of motion are given by Eqs.(2.16) after omission of the differential equation for Y and χ, and with $\chi = 0$:

$$\begin{aligned}
\dot{X} &= V \cos\gamma \\
\dot{h} &= V \sin\gamma \\
m\dot{V} &= T \cos\varepsilon - D - m\, g \sin\gamma \\
mV\dot{\gamma} &= (T \sin\varepsilon + L) \cos\mu - m\, g \cos\gamma \\
\dot{m} &= -\beta
\end{aligned} \tag{3.35}$$

Because this system is only valid for flight in the vertical plane, the sideslip angles and the sideforce Q have been set to zero. For a fixed engine this set has π, α and μ as control, where μ can only assume the value of 0 deg or +/- 180 deg. The bank angle for the Split-S maneuver, for instance, would be 180 deg all the way,

along with a heading angle of zero deg, and a flight path angle ranging from zero to - 180 deg. The real set of Euler angles is found by simply checking on $|\gamma| > 90$ deg and, if the test is positive, adding +/- 180 deg to χ and μ, and setting γ to its complement of +/- 180 deg using

$$\gamma = \frac{\gamma^*}{|\gamma^*|} \cdot \pi - \gamma^* \tag{3.36}$$

where $|\gamma^*| > 90$ deg is the flight path angle used in the integration.

This method will permit optimization of third-class trajectories with any parameter optimization method, as long as the trajectory can be flown in the vertical plane. Since this method is based on removing the $\dot{\chi}$ equation, it cannot work for three-dimensional flight.

4. Comparison

Three basic ideas have been presented that seem to remove the singularities that occur during integration of second- or third-class trajectories. For trajectories that can be flown in the vertical plane, the simple solution presented in the last section should be used. It is valid for third-class trajectories and allows a trajectory to be started in the vertical position without changing the algorithm. This method is also the easiest to set up among all those presented. In optimization problems where it is not known if the solution is a trajectory that can be flown in the vertical plane, one of the other methods has to be used.

To simplify the comparison of the remaining Euler-angle methods, they are referred to in the following as:

Method 1 - the inertial-acceleration method

Method 2 - the two-system method that uses yaw-pitch-roll Euler angles and that uses μ as control for both systems.

Method 3 - the two-system method that uses roll-pitch-yaw Euler angles for the set 2 equations.

Method 4 - the yaw-pitch-roll two-system method that uses ϕ as control while in set 2

If third-class trajectories can be excluded as possible solutions and only second-class trajectories are to be integrated, the inertial-acceleration method should be used, because it requires only one set of differential equations.

If third-class trajectories that include vertical rolls can be excluded as possible solution, method 4 should not be used because it is very restrictive and hard to set up. The choice of the right method among the remaining methods is not easy, however. Although only method 3 is valid for vertical flight in the strict mathematical sense, method 1 may be used also, as long as the trajectory is not started in the vertical position. Method 2 should not be used for third-class trajectories, because it does not allow trajectories to be as close to $\gamma = +/- 90$ deg as method 1 does. This is due to the fact that the $\sin\psi$ and $\sin\theta$ terms in the updating formula in method 2 become zero long before $\dot{X}$ and $\dot{Y}$ are zero. Whether method 1 or method 3 should be used for third-class trajectories will depend on the specific demands. Method 3 is harder to set up than method 1 because two sets of differential equations are used. Method 3 requires the assumption of zero roll rate while in the second set of equations. Both methods require an estimation when the vertical attitude is likely to be reached, but only method 1 requires the stepsize to be decreased and the integration to be stopped at $\gamma = -90$ deg. Method 3 may be started with vertical aircraft attitudes if the initial conditions are specified in the set 2 Euler angles, whereas method 1 cannot be started in the vertical position at all. Both methods will find the singularity in μ at $\gamma = -90$ deg themselves, and therefore, both can be used for parameter optimization if a dummy control is used.

If a rolling maneuver in the vertical position cannot be excluded as solution, the user should use the quaternion method which is derived in the next section. However, if the solution is almost known, method 4 may be used to find the exact solution.

Finally, it should be mentioned, that the user may combine any of the presented methods in a variety of ways to come up with better solutions. An easy implemented possibility could be a combination of the usual set of equations of motion as presented in Section II with the trivial solution of the last section. This would allow three-dimensional third-class trajectories to be integrated, as long as no roll at the vertical attitude has to be performed. It would allow rolls near the vertical attitude, however, just as with the inertial-acceleration method.

SECTION IV

THE QUATERNION METHOD

1. The Quaternion Concept

The use of three Euler angles to relate one coordinate system to another has the advantage of being well defined geometrically and fairly simple to visualize. The commonly used yaw-pitch-roll Euler angle sequence makes use of the fact that a system may be related to a reference system through the yaw angle and the pitch angle of its x-axis with respect to the reference system. It then only has to be rotated around its x-axis to achieve the desired orientation. It has been pointed out earlier that allowing the yaw and pitch angles both to assume values between - 180 deg and + 180 deg results in covering the globe twice. Hence, one angle has to be restricted. It was seen that this restriction leads to various problems which are relatively unpleasant to deal with.

The whole dilemma may be avoided if some other method of relating two coordinate systems is used. Here, the idea of using the quaternion comes into play. Although established by Hamilton as the general result of the division of two vectors, the main interest in quaternions today is focussed on its ability to relate two coordinate systems in a somewhat optimal way.

The reader will accept Euler's theorem, which states that any two coordinate systems with common origin can be aligned through one single rotation. This rotation takes place around an axis which passes through the common origin of both systems (see Figure 15). This axis is often referred to as the Euler axis. It is characterized by two vectors, one pointing in one direction of the axis, the other one in the opposite direction having merely an opposite sign. To get a complete description of the rotation, the angle through which the rotation takes place needs to be specified too. This means that a rotation of one system into another of common origin can be described by four parameters: one scalar for the rotation angle and three for the components of the vector pointing along the fixed rotation axis.

The quaternion is simply a compact form of representing this rotation angle and axis and consists of the sum of a scalar and a vector. It is given by

$$\underline{Q} = q_0 + \bar{q} = q_0 + [q_1, q_2, q_3]^T \; . \tag{4.1}$$

The scalar q_0 and the vector $\bar{q}$ are defined by

$$q_0 = \cos \frac{\theta}{2}$$

$$\bar{q} = \bar{\varepsilon} \sin \frac{\theta}{2} \tag{4.2}$$

where θ is the rotation angle that will be discussed in detail later and where $\bar{\varepsilon}$ is the vector pointing along the rotation axis, having the components ε_1, ε_2 and ε_3 in the reference system. This gives the

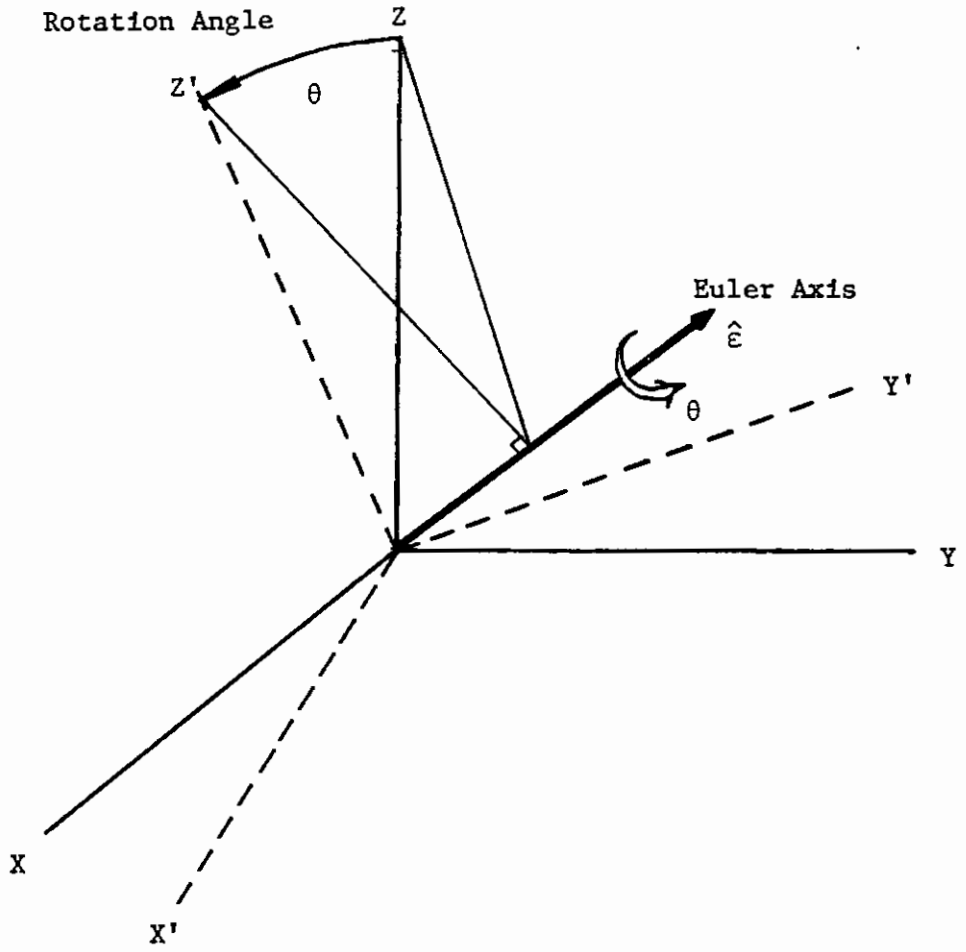

Figure 15 : Rotation Around the Euler Axis

quaternion elements $q_1 = \varepsilon_1 \sin\frac{\theta}{2}$, $q_2 = \varepsilon_2 \sin\frac{\theta}{2}$ and $q_3 = \varepsilon_3 \sin\frac{\theta}{2}$. If $\bar{\varepsilon}$ is a unit vector, i.e.

$$\varepsilon_1^2 + \varepsilon_2^2 + \varepsilon_3^2 = 1$$

then, and only then, the norm of the quaternion, which is defined in analogy to the vector norm, is given by

$$\underline{Q} = q_o^2 + q_1^2 + q_2^2 + q_3^2 = \cos^2\frac{\theta}{2} + \sin^2\frac{\theta}{2} = 1 \; . \qquad (4.3)$$

This special quaternion is called the unit quaternion or rotation quaternion. It will be seen in the next section that a unit quaternion rotates a vector into a vector of equal length, whereas arbitrary quaternions also stretch or contract vectors. Because only pure rotations are of interest here, only unit quaternions are considered in the following. For simplicity they will just be called quaternions.

Visualize again the rotation axis and the rotation angle. Let one direction of the rotation axis be defined through the unit vector $\hat{\varepsilon}_p$, and the other, through $\hat{\varepsilon}_n = -\hat{\varepsilon}_p$. Define the rotation angle θ to be positive in the mathematical positive sense, i.e. conforming to the right-hand rule. From Figure 16, it can now be seen that any rotation from one system (or vector) to some other system (or vector) may be described in four ways. These four possibilities are the following:

(a) - rotation around $\hat{\varepsilon}_p$ through the positive angle θ_{p1}

(b) - rotation around $\hat{\varepsilon}_p$ through the negative angle θ_{n1}, where $\theta_{n1} = -(2\pi - \theta_{p1})$

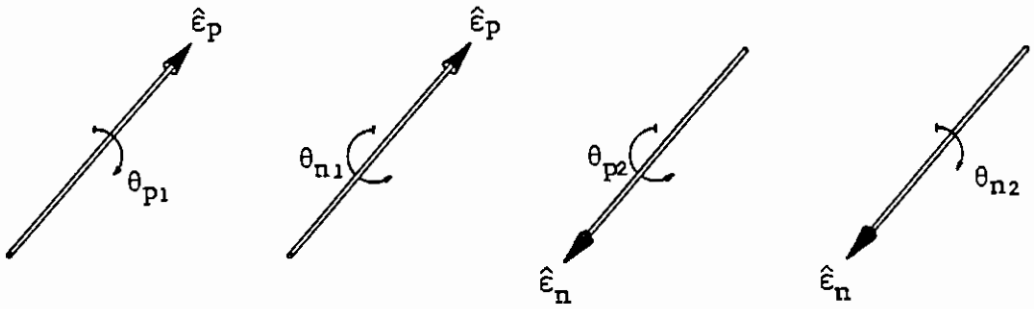

(a) (b) (c) (d)

Figure 16: Possible Rotations Around an Axis

(c) - rotation around $\hat{\varepsilon}_n$ through the positive angle θ_{p2}, where $\hat{\varepsilon}_n = -\hat{\varepsilon}_p$ and $\theta_{p2} = 2\pi - \theta_{p1}$

(d) - rotation around $\hat{\varepsilon}_n$ through the negative angle θ_{n2}, where $\theta_{n2} = -(2\pi - \theta_{p2}) = -\theta_{p1}$

It is immediately seen that cases (a) and (d) represent a physically identical rotation, just as the cases (b) and (c) do. Therefore two possibilities can be eliminated by allowing only positive rotation angles. This leaves the cases (a) and (c), which are characterized by positive rotation angles where one is less than 180 deg and the other one greater than 180 deg.

It is easy to establish the quaternion of a rotation for which the axis and the angle are known when using Eqs. (4.1) and (4.2). When using these equations, the quaternion for case (a) of Figure 16 is

given by

$$\underline{Q}_a = \cos\frac{\theta_{p1}}{2} + \hat{\varepsilon}_p \sin\frac{\theta_{p1}}{2} \tag{4.4}$$

whereas that for case (c) is given by

$$\underline{Q}_c = \cos\frac{\theta_{p2}}{2} + \hat{\varepsilon}_n \sin\frac{\theta_{p2}}{2} \ .$$

Substituting $\theta_{p2} = 2\pi - \theta_{p1}$ and $\hat{\varepsilon}_n = -\hat{\varepsilon}_p$ yields for $\underline{Q}_c$

$$\underline{Q}_c = -\cos\frac{\theta_{p1}}{2} - \hat{\varepsilon}_p \sin\frac{\theta_{p1}}{2} \tag{4.5}$$

where the relationships

$$\cos\frac{\theta_{p2}}{2} = \cos\left(\pi - \frac{\theta_{p1}}{2}\right) = -\cos\frac{\theta_{p1}}{2} \quad , \text{ and}$$

$$\sin\frac{\theta_{p2}}{2} = \sin\left(\pi - \frac{\theta_{p1}}{2}\right) = \sin\frac{\theta_{p1}}{2}$$

have been used. Comparison of $\underline{Q}_c$ as given in Eq. (4.5) with $\underline{Q}_a$ shows that the two quaternions which are associated with each rotation merely differ in the sign of their components. In other words, for every rotation of one vector into another two quaternions can be established if the rotation angle is restricted to positive angles: one for the rotation with a positive angle of less than 180 deg around one axis direction and a second one for the other rotation with an angle of more than 180 deg around the opposite axis direction. The two associated quaternions differ in the sign of their components. Furthermore, it is seen from the definition of the quaternion

$$\underline{Q} = \cos\frac{\theta}{2} + \hat{\varepsilon}\sin\frac{\theta}{2}$$

that the scalar part will remain nonnegative for all $0 \leq \theta \leq \pi$ (the rotation angle was restricted to positive values earlier). A quaternion with a nonzero scalar part is called a positive quaternion.

The ambiguity of having two quaternions for every aircraft attitude, i.e. the positive quaternion and the negative quaternion, may be removed by allowing only positive quaternions which amounts to the restriction $0 \leq \theta \leq \pi$. This would reduce the two remaining cases of Figure 16 to case (a). Allowing only positive quaternions makes sense in certain applications, as in spacecraft attitude control systems. There, the quaternion is used to find the minimum control that leads to a desired angular position of the spacecraft. Because the present orientation and the desired orientation of the vehicle are known, the two quaternions can be established. The positive quaternion will then give the minimum control because it gives the smaller rotation.

This property of the quaternion, however, is not of interest in this investigation. The quaternion is used here to describe aircraft attitudes in a singularity-free way, thus enabling integration of all possible aircraft attitudes. Restricting the quaternion to positive quaternions introduces singularities in the quaternion history for certain trajectories, as will be seen in the following.

Assume an aircraft flying straight and level rolls about the positive X - axis. The quaternion and bank angle histories for a horizontal roll is given in Figure 17, where the quaternion is restricted to the positive one. First, note that q_2 and q_3 stay zero for the entire time. This makes sense because the Euler axis for this trajectory coincides with the x-axis of the wind axes system and the reference system the entire time. For the first half roll the Euler axis points along the positive X - direction, and the q_1 curve is created through the multiplication with $\sin(\theta/2)$. For this half roll the rotation angle θ equals the bank angle μ. In the second half roll it becomes suddenly more "efficient" to rotate the reference system around the negative X - direction into the wind axes system, where the rotation angle is smaller than 180° and also positive. This causes the jump in q_1, which describes the axis orientation. It appears at first that such a singularity is unwanted. The consequence would be to allow positive and negative quaternions. If started out with the positive quaternion, the same rolling maneuver has the quaternion and bank angle history as shown in Figure 18. The singularities vanish, but the quaternion for the $\mu = 0$ attitude that is achieved after 1.0 s and one complete roll is now the negative counterpart of the initial quaternion. It should be stated that these plots have been generated using the quaternion representation of the equations of motion which is derived later in this section. The quaternion elements are found by integrating the quaternion differential equations. The continuous derivatives simply drive the

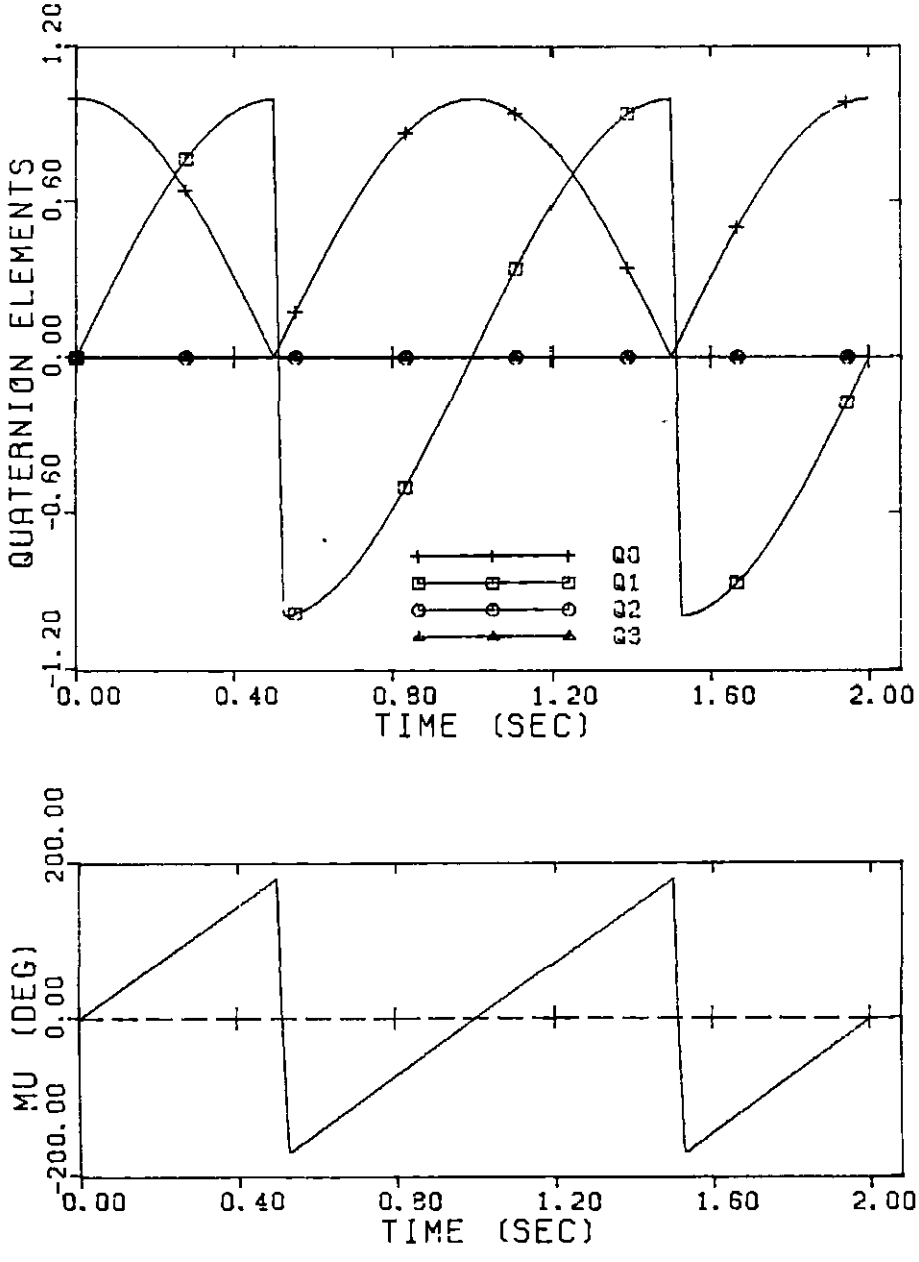

Figure 17 : Quaternion Element Histories for a Horizontal Roll with only Positive Quaternions

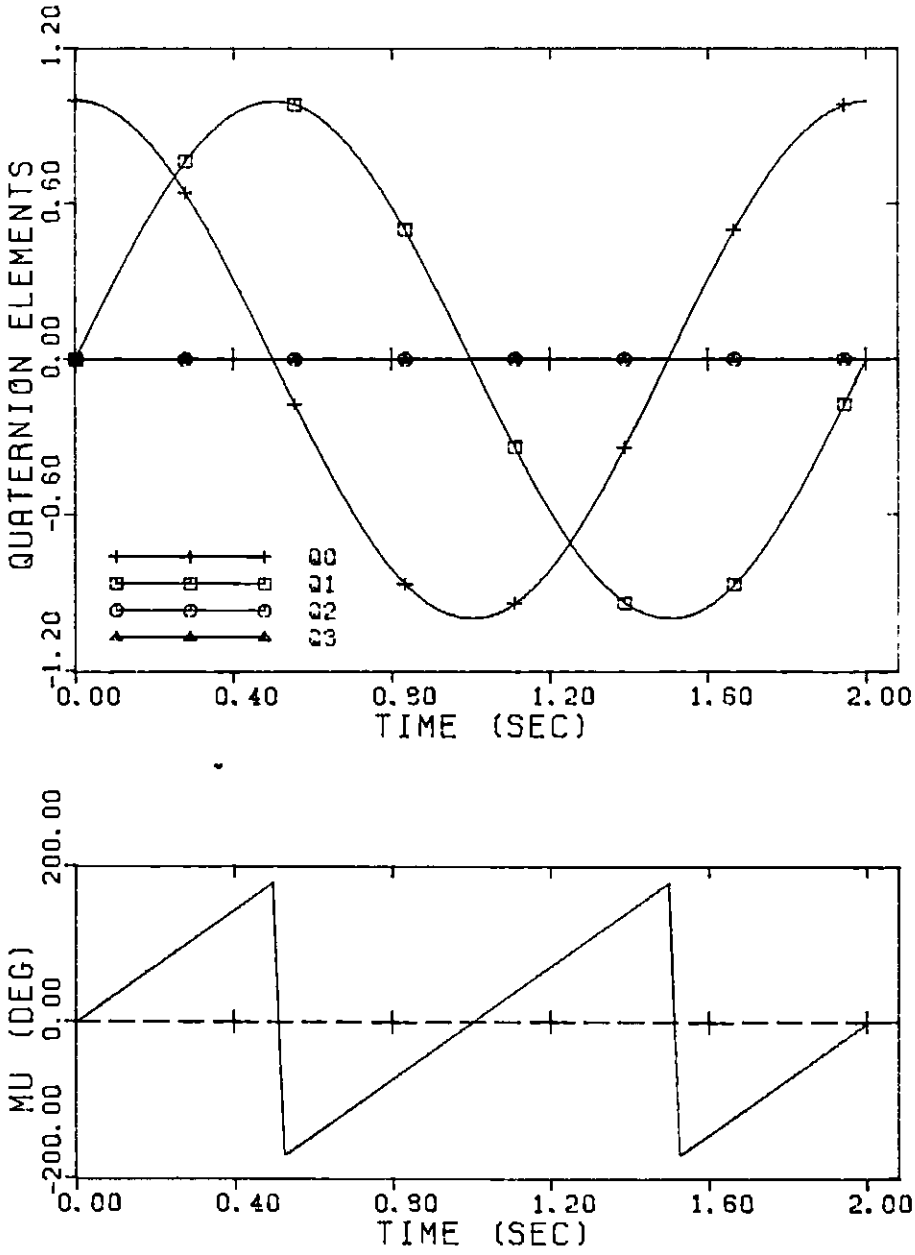

Figure 18 : Quaternion Element Histories for a Horizotal Roll Allowing Negative Quaternions

quaternion to be negative, ending up at the negative quaternion after one roll. This ambiguity is irrelevant, however. When starting the integration, the given initial Euler angles are converted to either quaternion, say the positive one. The integration is then carried out in the quaternion domain. Although two quaternions exist per aircraft attitude, only one aircraft attitude exists per quaternion. Therefore, the current Euler angles can be obtained at any point of the quaternion history.

In the case of parameter optimization, where final conditions have to be stated in terms of the quaternion elements, this ambiguity of having either the positive or the negative quaternion for every attitude does not create problems either. The final conditions are simply stated in terms of the positive quaternion and if the trajectory ends up with a negative quaternion, which is readily seen in the sign of q_o, then the signs of q_o through q_3 are changed, and the check is performed on the now positive final quaternion. How final conditions in terms of quaternion elements can be found will be explained at the end of Section IV.

The conclusion is that it does not matter whether the restriction on q_o is imposed or not. If the user wants to allow only positive quaternions, then the check on the sign of q_o has to be performed after every integration step. In that case the quaternion element histories have forced discontinuities as in Figure 17. These discontinuities compare to Euler angle discontinuities that result

from restrictions as $-\pi \leq \mu \leq +\pi$ as seen in Figure 17 (bottom). Since no problems arise when negative quaternions are allowed, the check on the sign of q_o after each integration step is unnecessary. The quaternion element histories are in that case continuous, and the check only has to be performed at the final point. This second possibility has been used by the author.

2.Quaternion Algebra

In this section the necessary quaternion algebra is presented. Due to the nature of this study, the desire to provide an easy understanding of the topic is emphasized, rather than giving complete mathematical proofs. Those can be found in Hamilton [2], as well as in various later publications.

2.1. Fundamental Operations

2.1.1. Identity

Two quaternions are identical iff all four elements are equal. Hence,

$$\underline{A} = \underline{B} \quad \text{iff} \quad a_o = b_o \quad \text{and} \quad \bar{a} = \bar{b} \ . \tag{4.6}$$

2.1.2. Quaternion Addition

If $\underline{A} = a_o + \bar{a}$, $\underline{B} = b_o + \bar{b}$ and $\underline{C} = c_o + \bar{c}$ are quaternions, then the addition of $\underline{A}$ and $\underline{B}$ is defined as

$$\underline{C} = \underline{A} + \underline{B} \tag{4.7}$$

where $c_o = a_o + b_o$ and $\bar{c} = \bar{a} + \bar{b}$.

2.1.3. Multiplication with a Scalar

If $\underline{A} = a_o + \bar{a}$ is a quaternion and s is a scalar, then

$$s\underline{A} = sa_o + s\bar{a} \ . \tag{4.8}$$

2.1.4. Quaternion Multiplication

Let the quaternions $\underline{Q}$ and $\underline{R}$ be given by

$$\underline{Q} = q_o + \bar{q} = q_o + q_1\hat{i} + q_2\hat{j} + q_3\hat{k}$$
$$\underline{R} = r_o + \bar{r} = r_o + r_1\hat{i} + r_2\hat{j} + r_3\hat{k}$$

where the unit vectors $\hat{i}$, $\hat{j}$ and $\hat{k}$ are assumed to follow Hamilton's "Fundamental Formula" [2, p.160]

$$\hat{i}^2 = \hat{j}^2 = \hat{k}^2 = \hat{i}\,\hat{j}\,\hat{k} = -1 , \tag{4.9}$$

which expands to

$$\begin{aligned} \hat{i}\,\hat{j} &= -\hat{j}\,\hat{i} = \hat{k} \\ \hat{j}\,\hat{k} &= -\hat{k}\,\hat{j} = \hat{i} \\ \hat{k}\,\hat{i} &= -\hat{i}\,\hat{k} = \hat{j} . \end{aligned} \tag{4.10}$$

Multiplying $\underline{Q}$ with $\underline{R}$ leads then to

$$\underline{Q}\,\underline{R} = (q_o + q_1\hat{i} + q_2\hat{j} + q_3\hat{k})\,(r_o + r_1\hat{i} + r_2\hat{j} + r_3\hat{k}) =$$

$$= q_o r_o - (q_1 r_1 + q_2 r_2 + q_3 r_3) + q_o(r_1\hat{i} + r_2\hat{j} + r_3\hat{k}) +$$

$$+ r_o(q_1\hat{i} + q_2\hat{j} + q_3\hat{k}) + \begin{vmatrix} \hat{i} & \hat{j} & \hat{k} \\ q_1 & q_2 & q_3 \\ r_1 & r_2 & r_3 \end{vmatrix} =$$

$$= q_o r_o - (q_1 r_1 + q_2 r_2 + q_3 r_3) + (q_o r_1 + q_1 r_o + q_2 r_3 - q_3 r_2)\hat{i}$$

$$+ (q_o r_2 + q_2 r_o + q_3 r_1 - q_1 r_3)\hat{j} + (q_o r_3 + q_3 r_o + q_1 r_2 - q_2 r_1)\hat{k}.$$

This can be written in vector form as

$$\underline{Q}\,\underline{R} = (q_o r_o - \bar{q} \cdot \bar{r}) + (q_o \bar{r} + r_o \bar{q} + \bar{q} \times \bar{r}) \qquad (4.11)$$

where $\bar{q} \cdot \bar{r}$ denotes the vector dot product and $\bar{q} \times \bar{r}$ the vector cross product. Note, that the first term in Eq. (4.11) is the scalar part of the resulting quaternion, and the second term, the vector part.

Since every vector is a special quaternion with zero scalar part, the unit vectors $\hat{i}$, $\hat{j}$ and $\hat{k}$ may be written as

$$\begin{aligned} \hat{i} &= \underline{i} = 0 + 1\hat{i} \\ \hat{j} &= \underline{j} = 0 + 1\hat{j} \\ \hat{k} &= \underline{k} = 0 + 1\hat{k} \,. \end{aligned} \qquad (4.12)$$

If Eq. (4.11) is now applied to Eqs. (4.12), then Eqs. (4.9) and (4.10), i.e. the assumptions on which (4.11) is based, are verified.

Close examination of Eq. (4.11) will reveal that quaternion multiplication is associative and distributive but because of the cross product generally not commutative. Note that Eq. (4.11) reduces for vectors to $\bar{q}\,\bar{r} = -\bar{q} \cdot \bar{r} + \bar{q} \times \bar{r}$, which gives the general vector multiplication resulting in a quaternion.

2.1.5. Conjugate

Because of the "imaginary" nature of the unit vectors as seen from Eqs. (4.9), it makes sense to define the conjugate of

$$\underline{Q} = q_o + \bar{p}$$

to be

$$\underline{Q}^* = q_o - \bar{q} \ . \tag{4.13}$$

With (4.11) this leads to the conjugate of a quaternion multiplication

$$(\underline{Q}\ \underline{R})^* = \underline{R}^*\underline{Q}^* \ . \tag{4.14}$$

Note that

$$(\underline{Q}^*)^* = \underline{Q} \ . \tag{4.15}$$

2.1.6. Norm

The norm of a quaternion is found like the norm for imaginary quantities by

$$\| \underline{Q} \| = \underline{Q}\ \underline{Q}^* = (q_o + \bar{q})(q_o - \bar{q}) = q_o^2 + \bar{q}\cdot\bar{q} =$$

$$= q_o^2 + q_1^2 + q_2^2 + q_3^2 \ . \tag{4.16}$$

Note that $\| \underline{Q} \| = 1$ for rotation quaternions.

2.1.7. Inverse

From (4.16) follows

$$\frac{\underline{Q}\underline{Q}^*}{\|\underline{Q}\|} = 1$$

which allows the inverse to be given by

$$\underline{Q}^{-1} = \frac{\underline{Q}^*}{\|\underline{Q}\|} . \tag{4.17}$$

For the rotation quaternion, where $\|\underline{Q}\| = 1$,

$$\underline{Q}^{-1} = \underline{Q}^* . \tag{4.18}$$

2.1.8. Derivative

The derivative of a quaternion is defined by

$$\frac{d\underline{Q}}{dt} = \frac{dq}{dt} + \frac{d\bar{q}}{dt} . \tag{4.19}$$

For a fixed coordinate system this equals

$$\frac{d\underline{Q}}{dt} = \frac{dq_0}{dt} + \frac{dq_1}{dt}\hat{i} + \frac{dq_2}{dt}\hat{j} + \frac{dq_3}{dt}\hat{k} .$$

2.2 Transformations Using Quaternions

A law is established that allows one vector to be rotated into another vector using a quaternion instead of a transformation matrix.

Consider the vector $\bar{p}$ with the components p_1, p_2 and p_3 in the coordinate system OXYZ. Rotate that vector through the angle θ around the Z-axis into the vector $\bar{p}'$, which has the same length as $\bar{p}$. Let $\hat{I}$, $\hat{J}$ and $\hat{K}$ be the unit-vectors along the X, Y and Z-axis respectively. Consider again the vectors to be special quaternions, and define

$$\underline{P} = 0 + \bar{p} = 0 + p_1\hat{I} + p_2\hat{J} + p_3\hat{K} \quad \text{and} \quad \underline{P}' = 0 + \bar{p}' \ .$$

It should be remembered that for every rotation for which the rotation axis and the rotation angle are known, a quaternion can be found. For the special rotation defined above, the quaternion rotating $\bar{p}$ into $\bar{p}'$ has its axis pointing along the Z-axis. The necessary quaternion is

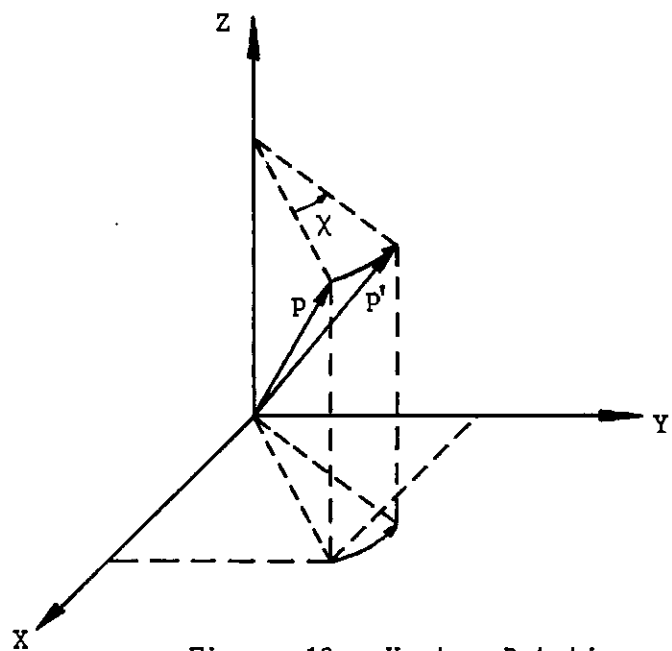

Figure 19 : Vector Rotation

found using Eqs. (4.2) and is given by

$$\underline{Q} = q_o + q_1\hat{I}\ q_2\hat{J} + q_3\hat{K} = \cos\frac{\theta}{2} + \sin\frac{\theta}{2}\hat{K} .$$

In appendix B is shown that $\underline{P}'$ is found using the formula

$$\underline{P}' = \underline{Q}\ \underline{P}\ \underline{Q}^* , \tag{4.20}$$

where $\underline{Q}^*$ is the quaternion conjugate of $\underline{Q}$ as defined in the previous section. Premultiplying (4.20) by $\underline{Q}^*$ and postmultiplying by $\underline{Q}$ gives

$$\underline{Q}^*\ \underline{P}'\ \underline{Q} = \underline{Q}^*\underline{Q}\ \underline{P}\ \underline{Q}^*\underline{Q} .$$

With Eq. (4.18) follows the inverse transformation

$$\underline{P} = \underline{Q}^*\ \underline{P}'\ \underline{Q} . \tag{4.21}$$

If the rotation around the Z-axis is visualized again, Eq. (4.21) makes sense. $\underline{P}$ is found by rotating $\underline{P}'$ through the angle $-\theta$ around the + Z-axis. $\underline{P}$ could also be found, however, by rotating $\underline{P}'$ through the angle $+\theta$ around the - Z-axis. For this rotation the quaternion rotating $\underline{P}'$ into $\underline{P}$ is then given by

$$q_o + q_3(-\hat{k}) = q_o - \bar{q} = \underline{Q}^* .$$

Applying this directly on Eq. (4.20) and using Eq. (4.15) gives

$$\underline{P} = \underline{Q}^*\ \underline{P}'\ (\underline{Q}^*)^*\ = \underline{Q}^*\ \underline{P}'\ \underline{Q} ,$$

which verifies (4.21).

Although Eq. (4.20) and Eq. (4.21) have been derived for the

special case of a rotation around the Z-axis, they are valid for every three-dimensonal rotation. It is known that every rotation can be defined by three Euler angles as defined in Section II.1. If $\underline{Q}_1$, $\underline{Q}_2$ and $\underline{Q}_3$ are the quaternions corresponding to the yaw, pitch and roll Euler angles χ, γ and μ respectively, the overall rotation of one vector $\underline{R}$ into another vector $\underline{R}'$ (of equal length) is given by the three rotations

$$\underline{R}_1 = \underline{Q}_1 \, \underline{R} \, \underline{Q}_1^*$$
$$\underline{R}_2 = \underline{Q}_2 \, \underline{R}_1 \, \underline{Q}_2^*$$
$$\underline{R}' = \underline{Q}_3 \, \underline{R}_2 \, \underline{Q}_3^* \, .$$

This simplifies to

$$\underline{R}' = \underline{Q}_3 \, \underline{Q}_2 \, \underline{Q}_1 \quad \underline{R} \quad \underline{Q}_1^* \, \underline{Q}_2^* \, \underline{Q}_3^*$$

and, after using (4.14), to

$$\underline{R}' = \underline{Q}_3\underline{Q}_2\underline{Q}_1 \, \underline{R} \, (\underline{Q}_3\underline{Q}_2\underline{Q}_1)^* \, . \qquad (4.22)$$

If $\underline{Q} = \underline{Q}_3\underline{Q}_2\underline{Q}_1$ is defined, where $\underline{Q}$ will generally have a rotation axis that does not point along a coordinate system axis, Eq. (4.20) is shown to be right for any $\underline{Q}$. Eq. (4.22) also states that the quaternion may be handled much the same as the direction cosine matrix, in that successive rotations result in successive quaternion multiplications. Because a multiplication of two quaternions takes less effort than the multiplication of two direction cosine matrices, extensive use of the quaternion is being made on the onboard Space Shuttle Computer System for attitude computations.

3. Some Necessary Relationships

In this section some relationships are developed that are needed to derive and work with the quaternion representation of the equations of motion, which will be derived in the next section.

3.1. A Coordinate Transformation Matrix Using Quaternions

A matrix will be needed later that relates one coordinate system to another coordinate system just like the direction cosine matrix but which is written in terms of elements of the corresponding transformation quaternion. The use of this matrix simplifies the transformation between two coordinate systems greatly over the use of the quaternion rotation formula as given by Eq. (4.20). It also leads to relationships between the quaternion elements and the Euler angles by comparing corresponding terms of the direction cosine matrix with terms of the quaternion matrix.

This matrix is found by rotating the unit vectors of the reference system into the unit vectors of the second system using Eq. (4.20). Let $\underline{Q}$ be the rotation quaternion that is defined in the reference system as

$$\underline{Q} = q_o + q_1\hat{I} + q_2\hat{J} + q_3\hat{K}$$

where $\hat{I}$, $\hat{J}$ and $\hat{K}$ are the unit vectors of the reference system. $\underline{Q}$ rotates the reference system into the second system in one rotation around the Euler axis. Thus, the unit vectors $\hat{i}$, $\hat{j}$ and $\hat{k}$ of the

second system are found according to Eq. (4.20) through the relationships

$$\hat{i} = \underline{Q}\,\hat{I}\,\underline{Q}^* \tag{4.23}$$

$$\hat{j} = \underline{Q}\,\hat{J}\,\underline{Q}^* \tag{4.24}$$

$$\hat{k} = \underline{Q}\,\hat{K}\,\underline{Q}^* \ . \tag{4.25}$$

For Eq. (4.23) this yields

$$\hat{i} = \underline{Q}\,\hat{I}\,(q_o - q_1\hat{I} - q_2\hat{J} - q_3\hat{K}) =$$

$$= (q_o + q_1\hat{I} + q_2\hat{J} + q_3\hat{K})(q_1 + q_o\hat{I} + q_3\hat{J} - q_2\hat{K}) =$$

$$= (q_oq_1 - q_1q_o - q_2q_3 + q_3q_2) + (q_o^2 + q_1^2 - q_2^2 - q_3^2)\hat{I} +$$
$$+ (q_oq_3 + q_1q_2 + q_3q_o + q_1q_2)\hat{J} + 2(q_1q_3 - q_oq_2)\hat{K} =$$

$$\hat{i} = (q_o^2 + q_1^2 - q_2^2 - q_3^2)\hat{I} + 2(q_oq_3 + q_1q_2)\hat{J} + 2(q_1q_3 - q_oq_2)\hat{K} \ .$$

Eqs. (4.24) and (4.25) are solved in a similar manner and result in

$$\hat{j} = 2(q_1q_2 - q_oq_3)\hat{I} + (q_o^2 - q_1^2 + q_2^2 - q_3^2)\hat{J} + 2(q_oq_1 + q_2q_3)\hat{K}$$

$$\hat{k} = 2(q_oq_2 + q_1q_3)\hat{I} + 2(q_2q_3 - q_oq_1)\hat{J} + (q_o^2 - q_1^2 - q_2^2 + q_3^2)\hat{K} \ .$$

This gives the desired transformation matrix

(4.26)

$$\begin{bmatrix} \hat{i} \\ \hat{j} \\ \hat{k} \end{bmatrix} = \begin{bmatrix} (q_o^2 + q_1^2 - q_2^2 - q_3^2) & 2(q_oq_3 + q_1q_2) & 2(q_1q_3 - q_oq_2) \\ 2(q_1q_2 - q_oq_3) & (q_o^2 - q_1^2 + q_2^2 - q_3^2) & 2(q_oq_1 + q_2q_3) \\ 2(q_oq_2 + q_1q_3) & 2(q_2q_3 - q_oq_1) & (q_o^2 - q_1^2 - q_2^2 + q_3^2) \end{bmatrix} \begin{bmatrix} \hat{I} \\ \hat{J} \\ \hat{K} \end{bmatrix}$$

This matrix may now be used just as the direction cosine matrix. It is orthogonal, and thus, its inverse is found by transposing it.

3.2. The Quaternion Differential Equation

Consider a vector $\bar{p}$ rotating with the angular velocity $\bar{\Omega} = p_{ref}\hat{I} + q_{ref}\hat{J} + r_{ref}\hat{K}$ relative to the reference system O X Y Z, and a fixed vector $\bar{r}$ that coincides with $\bar{p}$ at time $t = 0$, i.e., $\bar{r} = \bar{p}(0)$. Note, that for any time t a rotation may be established, which rotates $\bar{r}$ into $\bar{p}(t)$. Let $\underline{Q}(t)$ be the quaternion that defines this rotation from $\bar{r}$ to $\bar{p}(t)$. If $\underline{Q}_1$ denotes $\underline{Q}(t)$ and $\underline{Q}_2$ denotes $\underline{Q}(t + \Delta t)$, then

$$\bar{p}_1 = \bar{p}(t) = \underline{Q}_1 \, \bar{r} \, \underline{Q}_1^* \tag{4.27}$$

$$\bar{p}_2 = \bar{p}(t + \Delta t) = \underline{Q}_2 \, \bar{r} \, \underline{Q}_2^* \tag{4.28}$$

holds. According to Figure 20, the rotation $\underline{Q}_2$ can be split in two rotations. This yields

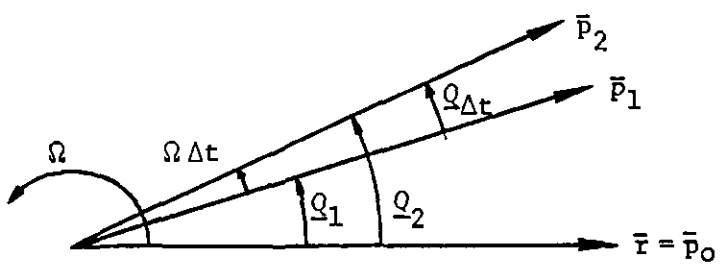

Figure 20 : Rotations Using Quaternions

$\bar{p}_1 = \underline{Q}_1 \bar{r} \underline{Q}_1^*$, and

$\bar{p}_2 = \underline{Q}_{\Delta t} \bar{p}_1 \underline{Q}_{\Delta t}^*$,

whereupon ,

$$\bar{p}_2 = \underline{Q}_{\Delta t} \underline{Q}_1 \bar{r} (\underline{Q}_{\Delta t} \underline{Q}_1)^*$$

which gives with Eq. (4.23)

$$\underline{Q}_2 = \underline{Q}_{\Delta t} \underline{Q}_1 \cdot \tag{4.29}$$

The quaternion $\underline{Q}_{\Delta t}$, which denotes the rotation from $\bar{p}_1$ to $\bar{p}_2$ can be specified because the rotation angle and rotation axis are known. With $\underline{Q} = \cos(\theta/2) + \hat{\varepsilon} \sin(\theta/2)$, where $\theta = \Omega \Delta t$ and where the axis $\hat{\varepsilon}$ is in the $\bar{\Omega}$ direction, $\underline{Q}_{\Delta t}$ is given by

$$\underline{Q}_{\Delta t} = \cos\frac{\Omega \Delta t}{2} + \frac{\bar{\Omega}}{\Omega} \sin\frac{\Omega \Delta t}{2} \tag{4.30}$$

The same rules of differentiation that are valid for scalars or vectors are valid for quaternions, as was shown in the last section. Thus, $\dot{\underline{Q}}$ may be found by

$$\dot{\underline{Q}}(t) = \lim_{\Delta t \to o} \frac{\underline{Q}(t + \Delta t) - \underline{Q}(t)}{\Delta t} \cdot \tag{4.31}$$

This yields with Eqs.(4.29) and (4.30)

$$\dot{\underline{Q}}_1 = \lim_{\Delta t \to o} \frac{\underline{Q}_2 - \underline{Q}_1}{\Delta t} = \lim_{\Delta t \to o} \frac{(\underline{Q}_{\Delta t} - 1)\underline{Q}_1}{\Delta t} =$$

$$= \lim_{\Delta t \to o} \left[\frac{1}{\Delta t} \left(\cos\frac{\Omega \Delta t}{2} - 1 + \frac{\bar{\Omega}}{\Omega} \sin\frac{\Omega \Delta t}{2} \right) \right] \underline{Q}_1 \cdot$$

Upon expression of $\cos\frac{\Omega\,\Delta t}{2}$ and $\sin\frac{\Omega\,\Delta t}{2}$ in Taylor series,

$$\dot{\underline{Q}}_1 = \lim_{\Delta t \to 0}\left[\frac{1}{\Delta t}\left(1 - \frac{(\Omega\Delta t)^2}{4\cdot 2!} + \ldots - 1 + \frac{\bar{\Omega}}{|\bar{\Omega}|}\left(\frac{\Omega\Delta t}{2} - \frac{(\Omega\,\Delta t)^3}{8\cdot 3!} + \ldots\right)\right)\right]\underline{Q}_1 \ .$$

and the sought differential equation is

$$\dot{\underline{Q}} = \frac{1}{2}\,\bar{\Omega}\,\underline{Q} \ . \tag{4.32}$$

This relates the angular velocity of some vector or coordinate system with respect to the reference system to the associated quaternion change. If the angular velocity is given in terms of the rotating system, a coordinate transformation has to be performed. Let $\bar{\omega} = p_w\hat{i} + q_w\hat{j} + r_w\hat{k}$ denote the angular velocity of some rotating system with respect to the reference system, where $\hat{i}$, $\hat{j}$ and $\hat{k}$ are the unit vectors of that rotating system. Then, the coordinate transformations are given by

$$\hat{i} = \underline{Q}\,\hat{I}\,\underline{Q}^*$$
$$\hat{j} = \underline{Q}\,\hat{J}\,\underline{Q}^*$$
$$\hat{k} = \underline{Q}\,\hat{K}\,\underline{Q}^* \ .$$

Since $\bar{\Omega}$ and $\bar{\omega}$ denote the same angular velocity vector, just expressed in different coordinate systems, $\bar{\Omega}$ is found from $\bar{\omega}$ using these transformations. Hence,

$$\bar{\omega}\Big/_{\substack{\text{ref.}\\ \text{system}}} = \bar{\Omega} = p_w\,\underline{Q}\,\hat{I}\,\underline{Q}^* + q_w\,\underline{Q}\,\hat{J}\,\underline{Q}^* + r_w\,\underline{Q}\,\hat{K}\,\underline{Q}^* \ .$$

The angular velocity components are scalars and can be brought inside

the transformation, if Eq.(4.8) is extended to the multiplication of a quaternion product with a scalar. This leads with the distributive property of the quaternion product to

$$\begin{aligned}\bar{\Omega} &= \underline{Q}\,(p_w\hat{I} + q_w\hat{J} + r_w\hat{K})\,\underline{Q}^* \\ &=: \underline{Q}\,\bar{\omega}_I\,\underline{Q}^*\end{aligned} \tag{4.33}$$

where $\bar{\omega}_I$ is a newly defined vector, which has the same components as $\bar{\omega}$, but is defined in the reference system. It is important to make the distinction between $\bar{\omega}$ and $\bar{\omega}_I$, because the quaternion could not operate on the vector $\bar{\omega}$, which has different unit vectors than the quaternion. Now Eq. (4.32) changes with Eq. (4.33) to

$$\dot{\underline{Q}} = \frac{1}{2}\,(\underline{Q}\,\bar{\omega}_I\,\underline{Q}^*)\,\underline{Q}$$

which gives the relationship between the angular velocity rates, as measured in the wind axes system, and the associated quaternion change, as

$$\dot{\underline{Q}} = \frac{1}{2}\,\underline{Q}\,\bar{\omega}_I\ . \tag{4.34}$$

Eq. (4.34) may now be expanded into four scalar equations for q_o through q_3 using the multiplication rule for quaternions. This yields immediately

$$\begin{aligned}\dot{q}_o &= -\,0.5\,(q_1p_w + q_2q_w + q_3r_w) \\ \dot{q}_1 &= \,0.5\,(q_op_w + q_2r_w - q_3q_w) \\ \dot{q}_2 &= \,0.5\,(q_oq_w + q_3p_w - q_1r_w) \\ \dot{q}_3 &= \,0.5\,(q_or_w + q_1q_w - q_2p_w)\ .\end{aligned} \tag{4.35}$$

3.3. Euler Angle to Quaternion Transformation

To derive a formula to compute the quaternion for given Euler angles, the rotation is split up in three Euler angles, and the quaternion for each rotation is established. The overall quaternion is then the product of these three provisional quaternions.

The transformation which corresponds to the velocity yaw-pitch-roll Euler angles transforms the horizontal reference system into the wind axes system through three consecutive rotations. The first rotation is around the z_h-axis into an intermediate system, call it system 1, the second one is around the y_1-axis into system 2 and the final rotation is around the x_2-axis into the wind axes system. Note, that x_2 and x_3 are identical. Let $\hat{I}$, $\hat{J}$ and $\hat{K}$ denote the unit vectors of the horizontal reference system, and $\hat{i}$, $\hat{j}$ and $\hat{k}$ be the unit vectors of the wind axes system. The quaternion $\underline{Q}_z$ for the first rotation around the z_h-axis is then given by

$$\underline{Q}_z = \cos\frac{\chi}{2} + \sin\frac{\chi}{2}\hat{K} = q_{zo} + q_{z3}\hat{K} \qquad (4.36)$$

where χ is the velocity yaw angle. The second rotation around the y_1-axis is represented by

$$\underline{Q}_y = \cos\frac{\gamma}{2} + \sin\frac{\gamma}{2}\hat{J}_1$$

where $\hat{J}_1$ can be expressed in terms of $\hat{I}$ and $\hat{J}$ using direction cosines

$$\hat{J}_1 = -\sin\chi\,\hat{I} + \cos\chi\,\hat{J} \ .$$

Hence,

$$\underline{Q}_y = \cos\frac{\gamma}{2} - \sin\frac{\gamma}{2}\sin\chi\,\hat{I} + \sin\frac{\gamma}{2}\cos\chi\,\hat{J} =$$
$$= q_{yo} + q_{y1}\hat{I} + q_{y2}\hat{J} \ . \qquad (4.37)$$

The final rotation is given by

$$\underline{Q}_x = \cos\frac{\mu}{2} + \sin\frac{\mu}{2}\,\hat{I}_2$$

where $\hat{I}_2$ can be stated as

$$\hat{I}_2 = \cos\gamma\,\hat{I}_1 - \sin\gamma\,\hat{K}_1 = \cos\gamma\,(\cos\chi\,\hat{I} + \sin\chi\,\hat{J}) - \sin\gamma\,\hat{K} \ .$$

Thus,

$$\underline{Q}_x = \cos\frac{\mu}{2} + \sin\frac{\mu}{2}\cos\gamma\cos\chi\,\hat{I} + \sin\frac{\mu}{2}\cos\gamma\sin\chi\,\hat{J} - \sin\frac{\mu}{2}\sin\gamma\,\hat{K} =$$
$$= q_{xo} + q_{x1}\hat{I} + q_{x2}\hat{J} + q_{x3}\hat{K} \ . \qquad (4.38)$$

In Section 2.2 of this chapter it has been shown, that the overall quaternion is found through successive multiplication of the component quaternions. Therefore,

$$\underline{Q} = q_o + q_1 + q_2 + q_3 = \underline{Q}_x\,\underline{Q}_y\,\underline{Q}_z \ .$$

This multiplication is carried out in Appendix C. It reduces to the following four Euler angle to quaternion relationships :

$$\begin{aligned}
q_o &= \cos\frac{\mu}{2}\cos\frac{\gamma}{2}\cos\frac{\chi}{2} + \sin\frac{\mu}{2}\sin\frac{\gamma}{2}\sin\frac{\chi}{2} \\
q_1 &= \sin\frac{\mu}{2}\cos\frac{\gamma}{2}\cos\frac{\chi}{2} - \cos\frac{\mu}{2}\sin\frac{\gamma}{2}\sin\frac{\chi}{2} \\
q_2 &= \cos\frac{\mu}{2}\sin\frac{\gamma}{2}\cos\frac{\chi}{2} + \sin\frac{\mu}{2}\cos\frac{\gamma}{2}\sin\frac{\chi}{2} \\
q_3 &= \cos\frac{\mu}{2}\cos\frac{\gamma}{2}\sin\frac{\chi}{2} - \sin\frac{\mu}{2}\sin\frac{\gamma}{2}\cos\frac{\chi}{2}
\end{aligned} \qquad (4.39)$$

3.4. Quaternion to Euler Angle Transformation

Because the equations of motion will be integrated in terms of the quaternion elements and it is desired to print out the results in terms of Euler angles, the transformation from quaternions to Euler angles is sought. It can be found by equating the direction cosine matrix, given by Eq. (2.4), to the quaternion matrix, given by Eq. (4.26). If the matrix elements (1,1), (1,2), (1,3), (2,3) and (3,3) are equated, the following relationships result :

$$\begin{aligned}
\sin\gamma &= 2\,(q_0q_2 - q_1q_3) && (1)\\
\cos\gamma\cos\chi &= q_0^2 + q_1^2 - q_2^2 - q_3^2 && (2)\\
\cos\gamma\sin\chi &= 2\,(q_0q_3 + q_1q_2) && (3)\\
\cos\gamma\cos\mu &= q_0^2 - q_0^2 - q_2^2 + q_3^2 && (4)\\
\cos\gamma\sin\mu &= 2\,(q_0q_1 + q_2q_3)\ . && (5)
\end{aligned} \qquad (4.40)$$

If the velocity pitch angle γ is restricted to the range $-\pi/2 \le \gamma \le +\pi/2$, a unique inverse sine value exists, and γ is found from (1) :

$$\gamma = \arcsin\ 2(q_0q_2 - q_1q_3)\ . \qquad (4.41)$$

The velocity yaw angle χ is given by (2) and (3) as

$$\chi = \arctan \frac{2\,(q_0q_3 + q_1q_2)}{q_0^2 + q_1^2 - q_2^2 - q_3^2}\ . \qquad (4.42)$$

Finally, the velocity roll angle μ results from (4) and (5)

$$\mu = \arctan \frac{2\,(q_0q_1 + q_2q_3)}{q_0^2 - q_1^2 - q_2^2 + q_3^2}\ . \qquad (4.43)$$

Because $q_o^2 + q_1^2 + q_2^2 + q_3^2 = 1$, Eqs. (4.42) and (4.43) simplify to

$$\chi = \arctan \frac{q_o q_3 + q_1 q_2}{0.5 - q_2^2 - q_3^2} \tag{4.44}$$

$$\mu = \arctan \frac{q_o q_1 + q_2 q_3}{0.5 - q_2^2 - q_1^2} \quad . \tag{4.45}$$

The full range of χ and μ will be found if the library function ATAN2(a,b) is used for evaluation of Eqs. (4.44) and (4.45).

The Euler angle to quaternion transformation formulas (4.39) and the reverse formulas (4.41), (4.44) and (4.45) have been checked numerically on a CDC Cyber 170 computer using single arithmetic. A set of Euler angles has been converted to the corresponding positive quaternion, which in turn has been transformed back into Euler angles after its norm had been computed. While the error in the norm always stayed on the order of 10^{-14}, the Euler angles were given back with an accuracy of over 10 digits for $|\gamma| < 89.99999$ deg. For larger fight path angles, the error in the Euler angles increased. The highest observed error occurs for $\gamma = +/- 90$ deg, where the returned χ and μ have an accuracy of at least one decimal place after the decimal point. Because the Euler angles are merely used for informational purposes to "see" the trajectory history, these minor errors have no influence on the accuracy of the program.

4. The Equations of Motion

The equations of motion in the quaternion representation are derived in much the same way as the equations in Section II, the only difference being that the quaternion transformation matrix (4.26) is used instead of the direction cosine matrix (2.4).

If the term for $\hat{i}_w$ is inserted from Eqs. (4.26), the kinematic equation

$$V\hat{i}_w = \dot{X}\hat{i}_h + \dot{Y}\hat{j}_h - \dot{h}\hat{k}_h$$

leads to the three scalar equations

$$\dot{X} = V\,(q_o^2 + q_1^2 - q_2^2 - q_3^2) \tag{4.46}$$

$$\dot{Y} = 2\,V\,(q_o q_3 + q_1 q_2) \tag{4.47}$$

$$\dot{h} = 2\,V\,(q_o q_2 - q_1 q_3)\,. \tag{4.48}$$

The only term that changes in the dynamic equations is the expression for the weight $\overline{W}$. With the transpose of Eqs. (4.26),

$$\overline{W} = mg\,\hat{k}_h$$

changes to

$$\overline{W} = 2\,mg\,(q_1 q_3 - q_o q_2)\hat{i}_w + 2\,mg\,(q_o q_1 + q_2 q_3)\hat{j}_w + \\ + mg\,(q_o^2 - q_1^2 - g_2^2 + q_3^2)\hat{k}_w\,. \tag{4.49}$$

Consequently, the force equation

$$m \frac{d\bar{V}}{dt} = \bar{T} + \bar{A} + \bar{W} ,$$

where $\bar{T}$ and $\bar{A}$ are given by Eqs. (2.7) and (2.8), respectively, results in the dynamic relationships

$$\dot{mV} = T \cos\varepsilon \cos\nu - D + 2 mg (q_1 q_3 - q_o q_2) \tag{4.50}$$

$$mVr_w = T \cos\varepsilon \sin\nu - Q + 2 mg (q_o q_1 + q_2 q_3) \tag{4.51}$$

$$mVq_w = T \sin\varepsilon + L - mg (q_o^2 - q_1^2 - q_2^2 + q_3^2) . \tag{4.52}$$

The quaternion elements q_o through q_3 have to be integrated simultaneously with the kinematic and the dynamic relationships using Eqs. (4.35). Collecting Eqs. (4.46) through (4.48), the dynamic relationships (4.50) through (4.52), the quaternion differential equations (4.35) and the mass equation, the equations of motion consist of the following set :

$$\begin{aligned}
\dot{X} &= V (q_o^2 + q_1^2 - q_2^2 - q_3^2) \\
\dot{Y} &= 2 V (q_o q_3 + q_1 q_2) \\
\dot{h} &= 2 V (q_o q_2 - q_1 q_3) \\
\dot{mV} &= T \cos\varepsilon \cos\nu - D + 2 mg (q_1 q_3 - q_o q_2) \\
\dot{q}_o &= - 0.5 (q_1 p_w + q_2 q_w + q_3 r_w) \\
\dot{q}_1 &= 0.5 (q_o p_w + q_2 r_w - q_3 q_w) \\
\dot{q}_2 &= 0.5 (q_o q_w + q_3 p_w - q_1 r_w) \\
\dot{q}_3 &= 0.5 (q_o r_w + q_1 q_w - q_2 p_w) \\
\dot{m} &= - \beta
\end{aligned} \tag{4.53}$$

where the velocity yaw rate r_w and the velocity pitch rate q_w are

given by

$$mVr_w = T\cos\varepsilon\sin\nu - Q + 2mg\,(q_0q_1 + q_2q_3)$$
$$mVq_w = T\sin\varepsilon + L - mg\,(q_0^2 - q_1^2 - q_2^2 + q_3^2) \quad .$$

If the engine is again assumed to be fixed and if the assumptions of zero sideslip angle σ and zero thrust sideslip angle ν are made, this set of differential equations has three mathematical degrees of freedom. Again, the power setting π and the angle of attack α or the lift coefficent C_L are controls. The interesting point is, however, that the velocity roll rate p_w is now the control instead of the bank angle μ.

The reader might get the idea, that the quaternion relationship

$$q_0^2 + q_2^2 + q_2^2 + q_3^2 = 1 \qquad (4.54)$$

should be included in the equations of motion, thus replacing one of the quaternion differential equations. This should not be done, because it would be hard to determine the sign of that quaternion element from Eq. (4.54), and it would also add the errors of three quaternion element integrations into the remaining element. It should also be realized that Eq. (4.54) is present in the equations of motion in an implicit form and is satisfied automatically. Examination of the equations of motion reveals the origin of the quaternion expressions present in Eqs. (4.53). Summing the squares of Eqs. (1), (2) and (3) and of Eqs. (1), (4) and (5) of Eqs. (4.40) proves this. However, it

is a good idea to scale every quaternion element by

$$C = \frac{1}{q_0^2 + q_1^2 + q_2^2 + q_3^2}$$

when the integration extends over many steps and integration errors start piling up. This scaling would of course occur between integration steps.

Having the roll rate p_w as the control will require some rethinking on the user's part. It will be seen in the next section, however, that this is a more "natural" control than the bank angle, because a constant bank angle does generally not correspond to a zero roll rate (remember Eqs. (2.15)). Note also, that the pilot controls directly the roll rate, not the bank angle.

5. Parameter Optimization Using the Quaternion Method

To help the reader get aquainted with the roll rate as control, the control history for two simple trajectories is analyzed. Then, the implementation of the quaternion method in parameter optimization is discussed.

The control for the Split-S maneuver is given by $p_w = 0$ deg/s all the way because the aircraft actually flies no roll at the vertical position even though the bank angle jumps from 180 deg to 0 deg at that point. The control for loops and Immelmanns is also $p_w = 0$ deg/s. A maneuver that yields a continuous bank angle change when flown with zero roll rate is the so-called "Lazy Eight", of which the first part is shown in Figure 21. Started with some bank angle, say 30 deg, a too high power setting or lift coefficient for a level turn will lead to a climbing turn. This increases the bank angle as long as the aircraft roll rate stays zero. The first of Eqs. (2.15),

$$p_w = \dot{\mu} - \dot{\chi} \sin\gamma \quad ,$$

confirms this. As the bank angle becomes steeper the flight path angle becomes shallower, which finally leads to the descending part. It is seen that this maneuver would be hard to simulate with μ as a control. It also follows that a climbing turn with constant bank angle will require a continuous nonzero roll rate. Hence, some trajectories with constant bank angle may be hard to simulate with p_w as a control. It is not possible to state generally if the roll rate history or the

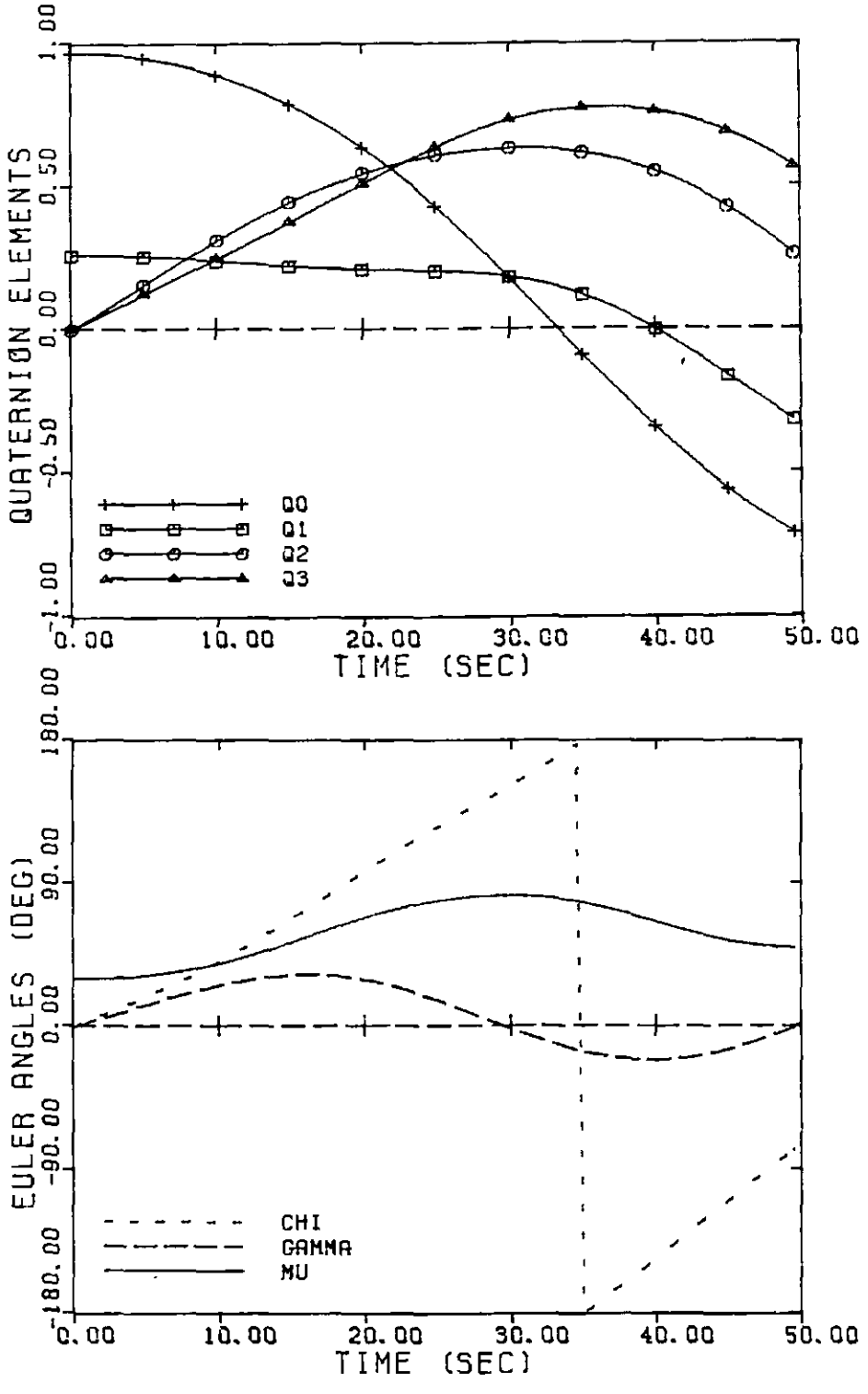

Figure 21 : Quaternion Element and Euler Angle Histories for a Lazy Eight

bank angle history is of an easier form. This depends on the specific trajectory being investigated. With these considerations in mind, it should not be too hard to come up with reasonable control guesses for optimization purposes.

Having the roll rate as a control has the big advantage of being able to perform rolls at any attitude. The disadvantage is, however, that now three nodal points are needed for a roll instead of only two points, as in bank angle controlled methods. The control history for a 180 deg roll is presented in Figure 22, where linear interpolation between nodal points again has been assumed. This

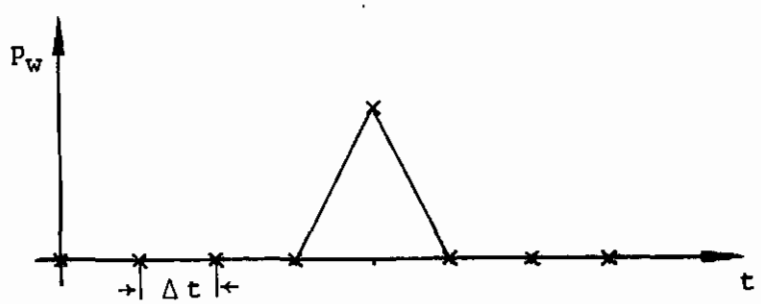

Figure 22 : Control History for a Roll

results in a quadratic bank angle change as shown in Figure 23. Note that an n^{th} order interpolation for p_w will result in an $(n+1)^{st}$ order function for μ. Hence, it takes two time intervals Δt to complete a roll, whereas a roll is completed after only one time interval for bank angle controlled methods, as seen from Figure 24.

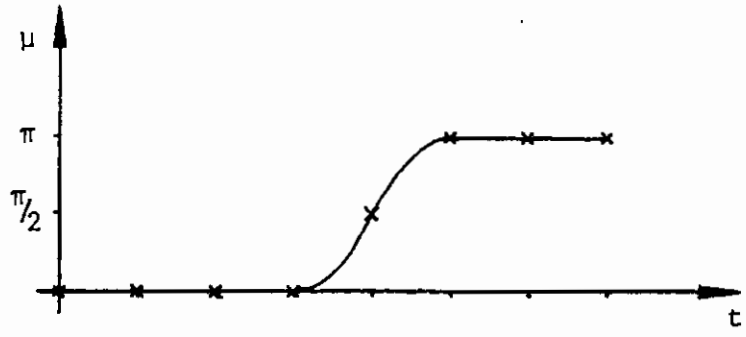

Figure 23 : Bank Angle History for a p_w-controlled Roll

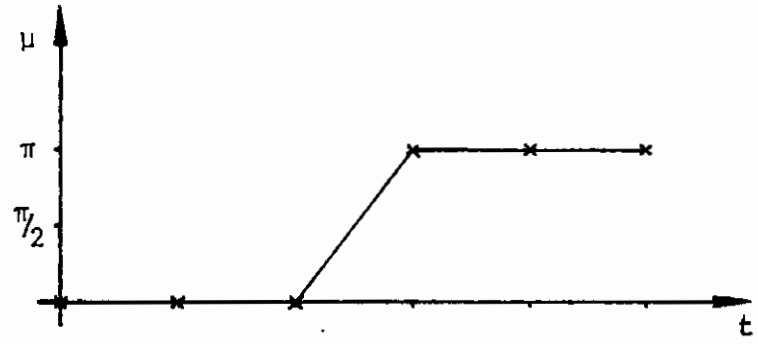

Figure 24 : Bank Angle History for a μ-controlled Roll

Therefore, the user might wish to increase the nodal point density if the trajectory includes several rolling maneuvers. This, however, is somewhat offset by the fact that only a $(n-1)^{st}$-order polynomial is required to achieve a n^{th}-order polynomial for the bank angle history in the case where the roll rate is the control. If on the other hand the order of nodal point interpolation is given, then the roll-rate-controlled method will result in a higher-order approximation of the bank angle.

When optimizing trajectories, the initial bank angle is usually left open because no initial constraints on the control are desired. This corresponds to an open initial roll rate in a roll rate controlled method. Nevertheless, it is desirable to be able to leave the initial bank angle even in such a method open. For the quaternion method this seems impossible at first, because the Euler angle to quaternion transformation requires the bank angle for every quaternion element. However, when the possible quaternion elements for a horizontal attitude with open bank angle are analyzed, a solution is readily found. This has already been done with the horizontal roll presented in Figure 17. Since q_2 and q_3 are zero for this case, q_o and q_1 have to follow the relationship

$$q_o^2 + q_1^2 = 1$$

which allows one element to be optimized. If the initial quaternion is required to be positive, i.e. $q_o \geq 0$, choosing q_1 between -1 and $+1$ will correspond to bank angles between $-$ 180 deg and $+$ 180 deg. The remaining quaternion element q_o is then computed from

$$q_o = + \sqrt{1 - q_1^2} \quad .$$

Hence, only one parameter, i.e. q_1, needs to be added to the parameter list if the initial bank angle is to be left open. If the initial attitude is fixed, the risk of losing at least two nodal points is taken if a roll has to be performed at the beginning of the trajectory. Note that two nodal points correspond to 2m parameters,

where m is the number of controls used.

To be able to state the final conditions in terms of quaternion elements, the same procedure as for the initial conditions has to be applied. The user has to analyze the possible quaternions to come up with some relationships which are then the final conditions. This may be done by a simple program that runs all possible Euler angle combinations and plots out the corresponding quaternions using Eq. (4.39). Often, especially if two final Euler angles are left unspecified, it is much quicker to analyze Eqs. (4.39) and (4.40) directly. If the final condition is $\gamma = 0$, with χ and μ being open, the first of Eqs. (4.40) gives the relationship

$$q_0 q_2 = q_1 q_3$$

which is now the final condition in terms of the quaternion elements.

Since it generally is not known if the trajectory ends up in a positive or in a negative quaternion, the final conditions have to be stated in terms of the positive quaternion. If a check on q_0 at the final point reveals a negative quaternion, the final quaternion has to be converted to a positive one before the final conditions can be applied. However, this check and conversion is unnecessary in many cases, as in the above example, where the final conditions do not change if the sign on all quaternion elements is changed simultaneously.

6. Discussion

A singularity-free method for integration of all third-class trajectories has been derived using quaternions. The differential equations for the Euler angles in the equations of motion are replaced by four differential equations for the quaternion elements. The bank angle is replaced by the roll rate p_w as control. This and the fact, that the integration is carried out with respect to quaternion elements instead of Euler angles causes some inconveniences for the user who wants to use this method for parameter optimization. Methods have been shown, however, for finding initial and final conditions in terms of quaternion elements. Having the roll rate as control might call for a slightly higher nodal point density if the trajectory includes several rolling maneuvers.

The method derived here is different from the quaternion method derived by Goodman [3]. Goodman replaces only the velocity yaw angle and the velocity pitch angle with the quaternion, which leaves the bank angle as control. Therefore, Goodman's method cannot solve the problems associated with the singularity in the bank angle that occurs at $\gamma = +/- 90$ deg. This makes the performance of Goodman's method comparable to that of the inertial-acceleration method, although the author did not test Goodman's method numerically.

A nice property of the quaternion method, which has not been mentioned yet, is its ability to give a cheap measure of the integration errors without having to use error controlled integrators.

Because the quaternion elements are found by integration, the sum of their squares will generally not equal exactly one. The integration error ε may therefore be indicated by

$$\varepsilon = q_0^2 + q_1^2 + q_2^2 + q_3^2 - 1$$

This integration error will depend on the actual quaternion change over the integrated time interval which in turn depends on the integration stepsize and the quaternion derivative. Because of the quaternion differential equation $\underline{\dot{Q}} = 0.5\, \underline{Q}\, \bar{\omega}_I$, the error will be a function of the stepsize Δt and the magnitude of the angular velocity, $\omega = |\bar{\omega}|$. Figure 25 shows the error ε versus the product of the stepsize and the magnitude of the angular velocity. This product gives the change in the angular position per integration step. It is seen from the plot, that in order to keep the integration error below, say, $\varepsilon = 10^{-9}$, the stepsize Δt has to be chosen such, that the aircraft attitude changes not more than 8 deg per integration step. Knowing ω from

$$\omega = \sqrt{p_w^2 + q_w^2 + r_w^2}$$

the stepsize is then computed from

$$\Delta t = \frac{x}{\omega}$$

where x is given from the plot for given ε. Although not obvious from Figure 25, it has been observed from print-outs that the error will stay in the truncation error range as long as the attitude change

does not exceed 1 deg per integration step. Only in that case may the quaternion normalization between integration steps be omitted as long as the total number of integration steps stays on the order of 10^2.

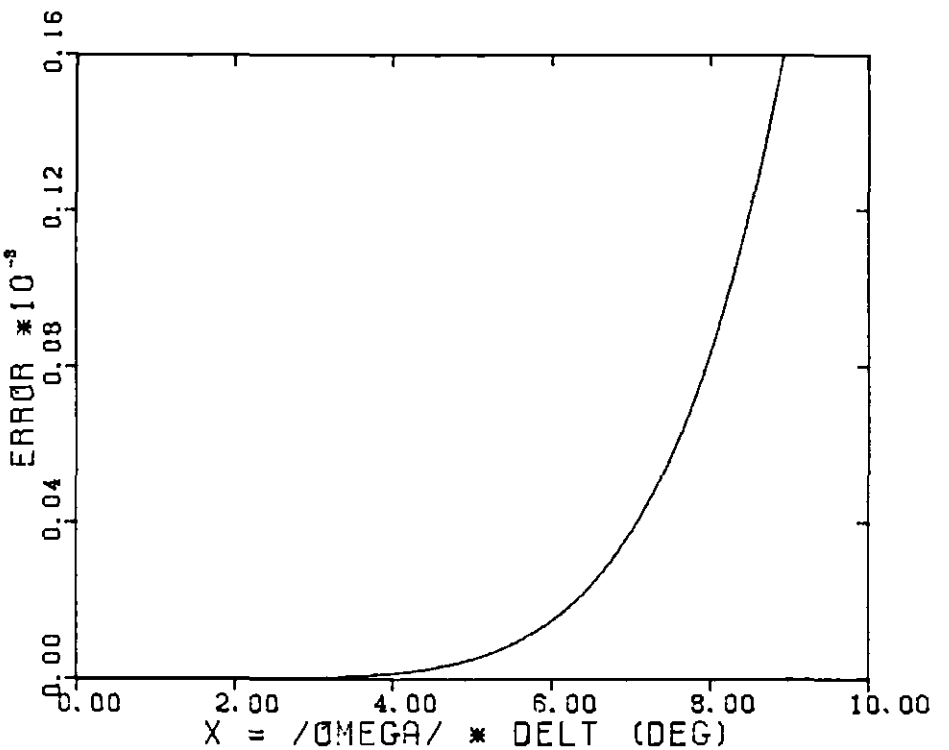

Figure 25 : Integraton Error per Integration Step for varying $\bar{\omega} \cdot \Delta t$

SECTION V

CONCLUSIONS

Several methods have been investigated that seem to remove the singularities associated with the integration of third-class trajectories. These methods can be devided into Euler-angle methods and the quaternion method. The Euler-angle methods are characterized by still requiring the bank angle as control whereas the quaternion method derived here has the roll rate as control. While all Euler-angle methods remove the singularity in the $\dot{\chi}$ equation of the commonly-used equations of motion, they cannot remove the singularity in μ. The only exceptions to this are the two-system method presented in Section III.2 that uses different bank angles as the controls for the two sets of differential equations and the method presented in Section III.3. While the former method is difficult to code and does not seem promising in cases where the user does not know exactly how the solution to his trajectory optimiztion problem might look like, the latter method is restricted to flight in the vertical plane. Whereas all presented μ-controlled Euler-angle methods are capable of dealing with second-class trajectories,they cannot handle every third-class trajectory. If third-class trajectories that involve not only vertical dives or climbs but also a rolling maneuver during those vertical dives or climbs are called fourth-class trajectories, then the following has been shown: none of the Euler-angle methods that use μ as control all the way is capable of integrating fourth-class

trajectories, whereas they may be used to integrate the remaining third-class trajectories in the practical sense. The reason for this lies in the fact, that the bank angle μ has to be 0 deg or 180 deg when hitting the vertical position as well as when departing from that position. A roll in the vertical position effectively reduces to a pure heading angle change where the bank angle has to be assumed constant, because it is the same before and after the rolling maneuver. Hence, no method that uses the bank angle μ as control all the way will be capable of controlling vertical rolls, i.e. fourth-class trajectories.

It has been shown that the quaternion method provides a singularity-free way for solving even fourth-class trajectory optimization problems, what Goodman [3] has not been able to show. Goodman replaces only the heading angle and the flight path angle with the quaternion, thus leaving the bank angle as control. In the method derived here all Euler angles are replaced by the quaternion, which leads to the roll rate as a control. This accounts for the controllability of fourth-class trajectories. After the user gets acquainted with having the roll rate as control, no problems should occur when optimizing trajectories with this method. Compared to some of the Euler-angle methods the quaternion method is easy to set up and can be used for all possible trajectories, whereas each Euler-angle method is restricted in the class of possible trajectories. The quaternion method has the further advantage of providing a cheap integration error control without having to use error controlled

integrators. Euler-angle-to-quaternion and quaternion-to-Euler-angle transformation formulas have been derived and it has been shown how to obtain initial and final conditions for the optimization in terms of the quaternion.

All derived methods and equations have been tested numerically on a CDC Cyber 170/750 computer system at the University of Texas at Austin. The author has not, however, implemented any of the presented methods in an actual parameter optimization problem. This should be done to verify the derived results, especially for the quaternion method.

APPENDIX A

The Equations of Motion for a Vertical Reference System Using a Roll-Pitch-Yaw Rotation Sequence

Let the reference system be the same vertical reference system as defined in Figure 13. Roll the reference system first around the $\hat{i}_v$-axis through the velocity roll angle ϕ into the intermediate system 1. Rotate then system 1 around its $\hat{j}_1$-axis through the velocity pitch angle θ into system 2. Finally, rotate system 2 about its $\hat{k}_2$-axis, which coincides with the $\hat{k}_w$-axis, through the velocity yaw angle ψ into the wind axes system. These partial transformations are described by the direction cosine matrices

$$\begin{bmatrix} \hat{i}_1 \\ \hat{j}_1 \\ \hat{k}_1 \end{bmatrix} = \begin{bmatrix} 1 & 0 & 0 \\ 0 & \cos\phi & \sin\phi \\ 0 & -\sin\phi & \cos\phi \end{bmatrix} \begin{bmatrix} \hat{i}_v \\ \hat{j}_v \\ \hat{k}_v \end{bmatrix} \tag{A.1}$$

$$\begin{bmatrix} \hat{i}_2 \\ \hat{j}_2 \\ \hat{k}_2 \end{bmatrix} = \begin{bmatrix} \cos\theta & 0 & -\sin\theta \\ 0 & 1 & 0 \\ \sin\theta & 0 & \cos\theta \end{bmatrix} \begin{bmatrix} \hat{i}_1 \\ \hat{j}_1 \\ \hat{k}_1 \end{bmatrix} \tag{A.2}$$

$$\begin{bmatrix} \hat{i}_w \\ \hat{j}_w \\ \hat{k}_w \end{bmatrix} = \begin{bmatrix} \cos\psi & \sin\psi & 0 \\ -\sin\psi & \cos\psi & 0 \\ 0 & 0 & 1 \end{bmatrix} \begin{bmatrix} \hat{i}_2 \\ \hat{j}_2 \\ \hat{k}_2 \end{bmatrix} \tag{A.3}$$

Multiplication of these matrices leads to the relationship between the vertical reference system and the wind axes system, which is given by

the direction cosine matrix

$$\begin{bmatrix} \hat{i}_w \\ \hat{j}_w \\ \hat{k}_w \end{bmatrix} = \begin{bmatrix} \cos\psi\cos\theta & \cos\psi\sin\theta\sin\phi + \sin\psi\cos\phi & -\cos\psi\sin\theta\cos\phi + \sin\psi\sin\phi \\ -\sin\psi\cos\theta & -\sin\psi\sin\theta\sin\phi + \cos\psi\cos\phi & \sin\psi\sin\theta\cos\phi + \cos\psi\sin\phi \\ \sin\theta & -\cos\theta\sin\phi & \cos\theta\cos\phi \end{bmatrix} \begin{bmatrix} \hat{i}_v \\ \hat{j}_v \\ \hat{k}_v \end{bmatrix} \quad (A.4)$$

The use of this direction cosine matrix reduces the kinematic equation

$$V\hat{i}_w = -\dot{X}\hat{k}_v + \dot{Y}\hat{j}_v - \dot{h}\hat{i}_v \quad .$$

to the scalar kinematic equations

$$\begin{aligned} \dot{X} &= V\,(\cos\psi\sin\theta\cos\phi - \sin\psi\sin\phi) \\ \dot{Y} &= V\,(\cos\psi\sin\theta\sin\phi + \sin\psi\cos\phi) \\ \dot{h} &= -V\cos\psi\cos\theta \quad . \end{aligned} \quad (A.5)$$

The dynamic equations are derived as in Section III.2.1, where the different relation for $\hat{i}_v$ in the weight equation should be remembered. This yields

$$m\dot{V} = T\cos\varepsilon\cos\nu - D + mg\cos\psi\cos\theta \quad (A.6)$$

$$mVr_w = T\cos\varepsilon\sin\nu - Q - mg\sin\psi\cos\theta \quad (A.7)$$

$$mVq_w = T\sin\varepsilon + L - mg\sin\theta \quad . \quad (A.8)$$

The yaw rate r_w and the pitch rate q_w are found from the equation for the angular velocity, which is given as

$$\bar{\omega} = p_w\hat{i}_w + q_w\hat{j}_w + r_w\hat{k}_w = \dot{\phi}\,\hat{i}_v + \dot{\theta}\,\hat{j}_1 + \dot{\psi}\,\hat{k}_2$$

where the intermediate system axes are related to the wind axes system by the matrix equation

$$\begin{bmatrix} \hat{i}_v \\ \hat{j}_1 \\ \hat{k}_2 \end{bmatrix} = \begin{bmatrix} \cos\theta\cos\psi & -\cos\theta\sin\psi & \sin\theta \\ \sin\psi & \cos\psi & 0 \\ 0 & 0 & 1 \end{bmatrix} \begin{bmatrix} \hat{i}_w \\ \hat{j}_w \\ \hat{k}_w \end{bmatrix} . \qquad (A.9)$$

This gives the angular rates

$$p_w = \dot{\phi}\cos\psi\cos\theta + \dot{\theta}\sin\psi \qquad (A.10)$$

$$q_w = -\dot{\phi}\sin\psi\cos\theta + \dot{\theta}\cos\psi \qquad (A.11)$$

$$r_w = \dot{\phi}\sin\theta + \dot{\psi} \; . \qquad (A.12)$$

It is seen that the needed equations for the yaw- and the pitch-rate involve the differentials of all three Euler angles. Therefore, the solution is not as trivial as in the case of yaw-pitch-roll Euler-angles. To solve Eqs. (A.10) through (A.12) along with Eqs. (A.7) and (A.8), one variable has to be picked as control. If Eqs. (A.10) through (A.12) are inverted, three differential equations for the Euler-angle rates $\dot{\psi}$, $\dot{\theta}$ and $\dot{\phi}$ result.

$$\begin{aligned} \dot{\psi} &= \frac{1}{\cos\theta}\left(-p_w\sin\theta\cos\psi + q_w\sin\psi\sin\theta + r_w\cos\theta\right) \\ \dot{\theta} &= q_w\cos\psi + p_w\sin\psi \\ \dot{\phi} &= \frac{1}{\cos\theta}\left(p_w\cos\psi - q_w\sin\psi\right) \end{aligned} \qquad (A.13)$$

These equations can now be integrated along with the other differential equations, if the terms for q_w and r_w are inserted from Eqs. (A.7) and (A.8) and if the roll rate p_w is picked as a control.

If the user is sure, that the trajectories being optimized do not include actual rolls during the time this set 2 is used, then the roll rate can be set to zero during this time interval. With this assumption the complete set of equations of motion is as follows :

$$
\begin{aligned}
\dot{X} &= V\,(\cos\psi \sin\theta \cos\phi - \sin\psi \sin\phi) \\
\dot{Y} &= V\,(\cos\psi \sin\theta \sin\phi + \sin\psi \cos\phi) \\
\dot{h} &= -V \cos\psi \cos\theta \\
m\dot{V} &= T \cos\varepsilon \cos\nu - D + mg \cos\psi\cos\theta \\
\dot{\psi} &= \frac{1}{\cos\theta}\,(q_w \sin\psi \sin\theta + r_w \cos\theta) \\
\dot{\theta} &= q_w \cos\psi \\
\dot{\phi} &= \frac{-1}{\cos\theta}\, q_w \sin\psi \\
\dot{m} &= -\beta
\end{aligned}
\qquad (A.14)
$$

where π and α (through $\varepsilon = \varepsilon_a + \alpha$) or C_L are the remaining controls and where r_w and p_w are given by Eqs. (A.7) and (A.8). Because p_w is set to zero, any control changes in μ will be ignored during the time this set of equations is used, although they are taken care of after switching back to system 1. Note that for every Split-S or Immelmann maneuver $\psi = 0$ deg or $\psi = 180$ deg, which lets the differential equation for ϕ vanish and which confirms the statement of constant ϕ for these maneuvers made in Section III.2.2. Whether or not $\dot{\phi}$ can actually be set to zero depends on the size of the time interval during which the set 2 equations are being used, and how closely the actual trajectory corresponds to a Split-S or Immelmann during that time.

The relationships between the two sets of Euler angles are found by comparing the appropriate terms that appear in the direction cosine matrices (2.4) and (A.4), while remembering the relationships between the two sets of unit vectors given in (3.9). This yields the nine equations

$$
\begin{aligned}
\cos\psi\cos\theta &= -\sin\gamma \\
\cos\psi\sin\theta\sin\phi + \sin\psi\cos\phi &= \cos\gamma\sin\chi \\
\cos\psi\sin\theta\cos\phi - \sin\psi\sin\phi &= \cos\gamma\cos\chi \\
-\sin\psi\cos\theta &= \sin\mu\cos\gamma \\
\cos\psi\cos\phi - \sin\psi\sin\theta\sin\phi &= \sin\mu\sin\gamma\sin\chi + \cos\mu\cos\chi \\
\sin\psi\sin\theta\cos\phi + \cos\psi\sin\phi &= \cos\mu\sin\chi - \sin\mu\sin\gamma\cos\chi \\
\sin\theta &= \cos\mu\cos\gamma \\
-\cos\theta\sin\phi &= \cos\mu\sin\gamma\sin\chi - \sin\mu\cos\chi \\
-\cos\theta\cos\phi &= \cos\mu\sin\gamma\cos\chi + \sin\mu\sin\chi \ .
\end{aligned}
\tag{A.15}
$$

The sought relationships are readily found. From set 1 to set 2 they are

$$\psi = \arctan\frac{-\sin\mu\cos\gamma}{-\sin\gamma} \tag{A.16}$$

$$\theta = \arcsin(\cos\mu\cos\gamma) \tag{A.17}$$

$$\phi = \arctan\frac{-\cos\mu\sin\gamma\sin\chi + \sin\mu\cos\chi}{-\cos\mu\sin\gamma\cos\chi - \sin\mu\sin\chi} \ . \tag{A.18}$$

Note again, that the negative signs in (A.16) and (A.18) should not be cancelled if ATAN2 is to find the right angle.

The reverse transformation, which gives the set 1 Euler angles back from the set 1 Euler angles, is given by the formulas

$$\chi = \arctan \frac{\cos\psi \sin\theta \sin\phi + \sin\psi \cos\phi}{\cos\psi \sin\theta \cos\phi - \sin\psi \sin\phi} \tag{A.19}$$

$$\gamma = - \arcsin (\cos\psi \cos\theta) \tag{A.20}$$

$$\mu = \arctan \frac{- \sin\psi \cos\theta}{\sin\theta} . \tag{A.21}$$

Appendix B

Transformations Using Quaternions

Proof of Equation (4.20)

The quaternions $\underline{P} = p_1\hat{I} + p_2\hat{J} + p_3\hat{K}$ and $\underline{Q} = \cos\frac{\chi}{2} + \sin\frac{\chi}{2}\hat{K}$ have been defined in Section IV.2.2. Postmultiply $\underline{P}$ by the quaternion conjugate $\underline{Q}^*$, and premultiply $\underline{P}\,\underline{Q}^*$ by the quaternion $\underline{Q}$. With the multiplication rule of Eq. (4.11) this leads to

$$\underline{Q}\,\underline{P}\,\underline{Q}^* = \underline{Q}\ (p_1\hat{I} + p_2\hat{J} + p_3\hat{K})(\cos\tfrac{\chi}{2} - \sin\tfrac{\chi}{2}\hat{K}) =$$

$$= (\cos\tfrac{\chi}{2} + \sin\tfrac{\chi}{2}\hat{K})\ p_3\sin\tfrac{\chi}{2} + (p_1\cos\tfrac{\chi}{2} - p_2\sin\tfrac{\chi}{2})\ \hat{I} +$$
$$+ (p_2\cos\tfrac{\chi}{2} + p_1\sin\tfrac{\chi}{2})\ \hat{J} + p_3\cos\tfrac{\chi}{2}\hat{K} =$$

$$= (p_1\cos^2\tfrac{\chi}{2} - 2\,p_2\sin\tfrac{\chi}{2}\cos\tfrac{\chi}{2} - p_1\sin^2\tfrac{\chi}{2})\ \hat{I} +$$
$$+ (p_2\cos^2\tfrac{\chi}{2} + 2\,p_1\sin\tfrac{\chi}{2}\cos\tfrac{\chi}{2} - p_2\sin^2\tfrac{\chi}{2})\ \hat{J} + p_3\hat{K}\ . \quad (B.1)$$

With the trigonometric identities

$$\cos^2\tfrac{\chi}{2} = 0.5\ (1 + \cos\chi) \quad (B.2)$$

$$\sin^2\tfrac{\chi}{2} = 0.5\ (1 - \cos\chi) \quad (B.3)$$

$$2\sin\tfrac{\chi}{2}\cos\tfrac{\chi}{2} = \sin\chi\ , \quad (B.4)$$

Eq. (B.1) simplifies to

$$\underline{Q}\,\underline{P}\,\underline{Q}^* = (p_1\cos\chi - p_2\sin\chi)\hat{I} + (p_2\cos\chi + p_1\sin\chi)\hat{J} + p_3\hat{K}\ . \quad (B.5)$$

To show that the operation $\underline{Q}\,\underline{P}\,\underline{Q}^*$ is really the operation that rotates the vector $\bar{p}$ into the vector $\bar{p}'$, $\bar{p}$ can be rotated using a direction cosine matrix, and the result, compared with that of Eq. (B.5). This rotation is given by

$$\bar{p}' = \begin{bmatrix} \cos\chi & -\sin\chi & 0 \\ \sin\chi & \cos\chi & 0 \\ 0 & 0 & 1 \end{bmatrix} \bar{p} \qquad (B.6)$$

which expands to

$$\bar{p}' = (p_1\cos\chi - p_2\sin\chi)\hat{I} + (p_1\sin\chi + p_2\cos\chi)\hat{J} + p_3\hat{K} \qquad (B.7)$$

Comparison of Eq. (B.7) with (B.5) proves Eq. (4.20), that is,

$$\underline{P}' = \underline{Q}\,\underline{P}\,\underline{Q}^* , \qquad (B.7)$$

for the case where $\underline{P}$ and $\underline{P}'$ are vectors. The case where both are general quaternions is not of interest, since a vector transformation is sought, and it is known anyway that quaternion multiplications result generally in quaternions. That Eq. (B.7) holds for any quaternion $\underline{Q}$ and not only for the special quaternion considered above is shown in Section IV.2.2.

APPENDIX C

Euler-Angle-To-Quaternion Transformation

To derive Eqs. (4.39), the multiplication $\underline{Q}_x\underline{Q}_y\underline{Q}_z$ has to be carried out, where $\underline{Q}_x$, $\underline{Q}_y$ and $\underline{Q}_z$ are given by Eqs. (4.36), (4.37) and (4.38) respectively. With the multiplication rule of Eq.(4.11) this gives

$$\underline{Q} = \underline{Q}_x \{q_{yo} + q_{y1}\hat{I} + q_{y2}\hat{J})(q_{zo} + q_{z3}\hat{K})\} =$$

$$= \underline{Q}_x \{q_{yo}q_{zo} + q_{zo}q_{y1}\hat{I} + q_{zo}q_{y2}\hat{J} + q_{yo}q_{z3} + \begin{vmatrix} \hat{I} & \hat{J} & \hat{K} \\ q_{y1} & q_{y2} & 0 \\ 0 & 0 & q_{z3} \end{vmatrix}\} =$$

$$= (q_{xo} + q_{x1}\hat{I} + q_{x2}\hat{J} + q_{x3}\hat{K})\{q_{yo}q_{zo} + (q_{zo}q_{y1} + q_{y2}q_{z3})\hat{I} +$$

$$+ (q_{zo}q_{y2} - q_{y1}q_{z3})\hat{J} + q_{yo}q_{z3}\hat{K}\} . \quad (C.1)$$

This leads to Eq. (C.2)

$$\underline{Q} = q_{xo}q_{yo}q_{zo} - q_{x1}q_{zo}q_{y1} - q_{x1}q_{y2}q_{z3} - q_{x2}q_{zo}q_{y2} + q_{x2}q_{y1}q_{z3} - q_{x3}q_{yo}q_{z3} +$$

$$(q_{xo}q_{zo}q_{y1} + q_{xo}q_{y2}q_{z3} + q_{x1}q_{yo}q_{zo} + q_{x2}q_{yo}q_{z3} - q_{x3}q_{zo}q_{y2} + q_{x3}q_{y1}q_{z3})\hat{I} +$$

$$(q_{xo}q_{zo}q_{y2} - q_{xo}q_{y1}q_{z3} + q_{x2}q_{yo}q_{zo} - q_{x1}q_{yo}q_{z3} + q_{x3}q_{zo}q_{y1} + q_{x3}q_{y2}q_{z3})\hat{J} +$$

$$(q_{xo}q_{yo}q_{z3} + q_{x3}q_{yo}q_{zo} + q_{x1}q_{zo}q_{y2} - q_{x1}q_{y1}q_{z3} - q_{x2}q_{zo}q_{y1} - q_{x2}q_{y2}q_{z3})\hat{K} .$$

The terms for the q_{xi}, q_{yi} and q_{zi} are found from Eqs. (4.36) through (4.38) and inserted in Eq. (C.2). With the trigonometric

identities

$$\cos\chi = \cos^2\frac{\chi}{2} - \sin^2\frac{\chi}{2} \quad , \quad \sin\chi = 2\sin\frac{\chi}{2}\cos\frac{\chi}{2}$$
$$\cos\gamma = \cos^2\frac{\gamma}{2} - \sin^2\frac{\gamma}{2} \quad , \quad \sin\gamma = 2\sin\frac{\gamma}{2}\cos\frac{\gamma}{2} \qquad (C.3)$$

and the fundamental relationship

$$\underline{Q} = q_o + q_1\hat{I} + q_2\hat{J} + q_3\hat{K} \ ,$$

Eq. (C.2) leads to the four scalar equations

$$\begin{aligned}
q_o &= \cos\frac{\mu}{2}\cos\frac{\gamma}{2}\cos\frac{\chi}{2} + \sin\frac{\mu}{2}\sin\frac{\gamma}{2}\sin\frac{\chi}{2} \\
q_1 &= \sin\frac{\mu}{2}\cos\frac{\gamma}{2}\cos\frac{\chi}{2} - \cos\frac{\mu}{2}\sin\frac{\gamma}{2}\sin\frac{\chi}{2} \\
q_2 &= \cos\frac{\mu}{2}\sin\frac{\gamma}{2}\cos\frac{\chi}{2} + \sin\frac{\mu}{2}\cos\frac{\gamma}{2}\sin\frac{\chi}{2} \\
q_3 &= \cos\frac{\mu}{2}\cos\frac{\gamma}{2}\sin\frac{\chi}{2} - \sin\frac{\mu}{2}\sin\frac{\gamma}{2}\cos\frac{\chi}{2} \ .
\end{aligned} \qquad (C.4)$$

BIBLIOGRAPHY

1. Miele, Angelo, "Flight Mechanics I, Theory of Flight Paths", Addison-Wesley, Reading, Mass., 1962

2. Hamilton, Sir William Rowan, "Elements of Quaternions, Vol.I", 3rd edition, Chelsea, New York, 1969

3. Goodman, Richard, J., "Digital Simulation of Aircraft Flight Path Dynamics Using Quaternions", AIAA Paper 78-311

4. Well, Karl, H., "Optimization of Tactical Aircraft Maneuvers Utilizing High Angles of Attack", AIAA Paper 80-1596

5. Sunkel, J.,W., and Peters, W., H., "Quaternions for Control of the Space Shuttle", NASA JSC-Internal Note, JSC-11150

6. Hull, David, G., "Numerical Methods in Optimal Control", Class Notes, the University of Texas at Austin, Spring 1981

7. Fletcher, R., "An Ideal Penalty Function for Constrained Optimization", J. Inst. Maths Applics Vol. 15, pp 319-342, 1975

The vita has been removed from the digitized version of this document.